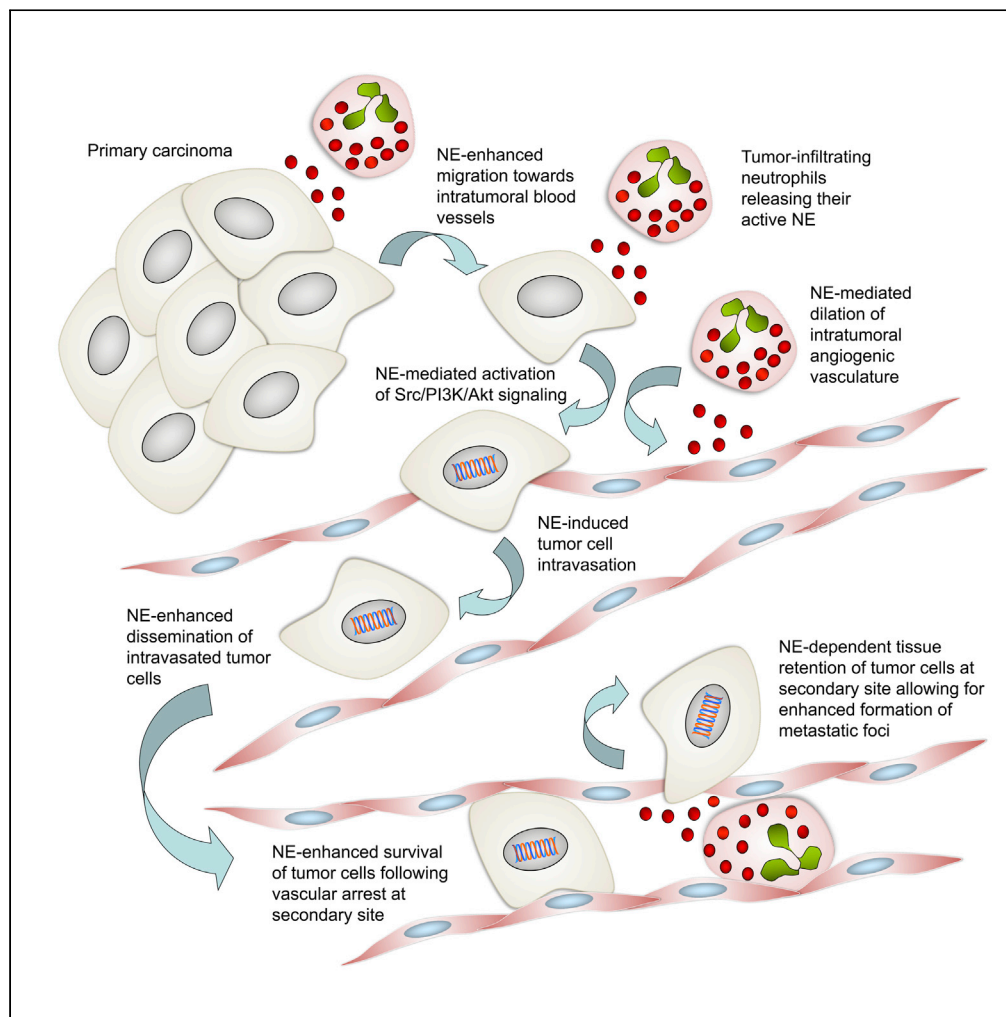# iScience

Article

Neutrophil Elastase Facilitates Tumor Cell Intravasation and Early Metastatic Events

Elena Deryugina, Alexia Carré, Veronica Ardi, Tomoki Muramatsu, Jonas Schmidt, Christine Pham, James P. Quigley

deryugin@scripps.edu (E.D.)
jquigley@scripps.edu (J.P.Q.)

HIGHLIGHTS

NE enhances human carcinoma cell intravasation and spontaneous metastasis

NE mediates formation of dilated intratumoral vasculature supporting cell intravasation

NE-KO mice exhibit decreased lung retention and spontaneous metastasis of tumor cells

NE induces tumor cell survival and migration via activation of Src/PI3K/Akt pathway

Article

Neutrophil Elastase Facilitates
Tumor Cell Intravasation
and Early Metastatic Events

Elena Deryugina,[1,7,*] Alexia Carré,[1,4] Veronica Ardi,[1,2] Tomoki Muramatsu,[1,5] Jonas Schmidt,[1,6] Christine Pham,[3] and James P. Quigley[1,*]

SUMMARY

Functional roles of neutrophil elastase (NE) have not been examined in distinct steps of the metastatic cascade. NE, delivered to primary tumors as a purified enzyme or within intact neutrophils or neutrophil granule content, enhanced human tumor cell intravasation and subsequent dissemination via NE-mediated formation of dilated intratumoral vasculature. These effects depended on picomole range of NE activity, sensitive to its natural inhibitor, α1PI. In *Elane*-negative mice, the lack of NE decreased lung retention of human tumor cells in experimental metastasis. Furthermore, NE was essential for spontaneous metastasis of murine carcinoma cells in a syngeneic orthotopic model of oral cancer. NE also induced tumor cell survival and migration via Src/PI3K-dependent activation of Akt signaling, vital for tumor cell dissemination *in vivo*. Together, our findings implicate NE, a potent host enzyme specific for first-responding innate immune cells, as directly involved in early metastatic events and a potential target for therapeutic intervention.

INTRODUCTION

Cancer progression involves several distinct steps associated with heightened activity of tumor-associated neutrophils. Tumor cells secrete cytokines and chemokines that attract inflammatory leukocytes and myeloid-derived suppressor cells (MDSCs) (Coffelt et al., 2016; Gonzalez et al., 2018; Taniguchi and Karin, 2018). In response to cytokines emanating from a growing tumor, the bone marrow increases production of neutrophils and MDSCs, which egress into blood circulation, reach the primary tumor site, and infiltrate the tumor environment (Marvel and Gabrilovich, 2015; Ouzounova et al., 2017; Zhou et al., 2018). The increased numbers of circulating neutrophils and their granulocytic counterparts closely correlate with tumor progression and reduced patient survival in a variety of human malignancies, suggesting that cancer likely adapts the host-protective innate immune system to facilitate tumor growth and metastasis (Crusz and Balkwill, 2015; Dongre and Weinberg, 2019).

Being the first leukocytes to infiltrate a developing tumor, the neutrophilic granulocytes play an important role in coordinating inflammatory responses beyond their established role in pathogen elimination (Henry et al., 2016; Mantovani et al., 2011; Mocsai, 2013). Mature neutrophils become an essential part of the tumor microenvironment (Jodele et al., 2006), by releasing their secretory granules containing potent enzymes and, in some cases, generating extracellular traps (NETs) (Albrengues et al., 2018; Liang and Ferrara, 2016; Nicolas-Avila et al., 2017; Powell and Huttenlocher, 2016). Certain neutrophil-derived proteases can functionally activate or modify a number of proteins, which induce tumor cell survival and motility and trigger the angiogenic switch, all prerequisites for tumor growth and metastasis (Ardi et al., 2007, 2009; Kessenbrock et al., 2010; Nozawa et al., 2006). In particular, neutrophil MMP-9, a structurally and functionally unique form of MMP-9, was demonstrated to liberate from the extracellular matrix a number of direct angiogenic factors, such as VEGF and basic FGF, making them available to activate endothelial cells and induce tumor angiogenesis (Ardi et al., 2009; Shojaei et al., 2008). Tumor-infiltrating neutrophils contribute to MMP-9-dependent attraction of pericytes and development of an intratumoral vasculature crucial for efficient hematogenous dissemination of cancer cells (Chantrain et al., 2004; Jodele et al., 2005). An intimate cooperation between disseminating tumor cells and influxing neutrophils was shown to be critical also for the steps of metastasis following the initial intravasation step (Labelle and Hynes, 2012). In a remarkable reciprocal manner, tumor cells modulate the cytokines that attract host neutrophils and activate neutrophil-mediated signaling pathways facilitating cancer metastasis (Huh et al., 2010; Opdenakker et al.,

[1]Department of Molecular Medicine, The Scripps Research Institute, 10550 North Torrey Pines Road, La Jolla, CA 92037, USA

[2]National University, 9388 Lightwave Avenue, San Diego, CA 92123, USA

[3]Department of Internal Medicine, Washington University, St. Louis, MO 63110, USA

[4]Present address: Université de Paris, Institut Cochin, INSERM, CNRS, 75014 Paris, France

[5]Present address: Department of Molecular Cytogenetics, Medical Research Institute, Tokyo Medical and Dental University, Tokyo, Japan

[6]Present address: Department of Pharmacy, Goethe-University, Max-von-Laue-Str. 9, 60438, Frankfurt am Main, Germany

[7]Lead Contact

*Correspondence: deryugin@scripps.edu (E.D.), jquigley@scripps.edu (J.P.Q.)

https://doi.org/10.1016/j.isci.2020.101799

2001; Strell et al., 2010; Tam et al., 2004). In addition to MMP-9, inflammatory neutrophils carry a cargo of other proteases, including cathepsin G, proteinase 3, and neutrophil elastase (NE), which play critical roles in chronic inflammation and acute responses to infection and injury (Korkmaz et al., 2010; Pham, 2006).

Among neutrophil-specific serine proteases, neutrophil-derived NE is of interest because of its unique potency to escalate immune responses, microbial elimination, and wound repair (Kettritz, 2016; Stapels et al., 2015). Although some reports describe the detection of NE in non-neutrophilic cell types (Sato et al., 2006), high levels of NE protein and NE activity have been demonstrated almost exclusively in neutrophils and their released granule contents. Therefore, it is not surprising that the heightened presence of NE and neutrophils often overlap in pathological conditions involving neutrophil influx into inflamed tissues. Accumulating evidence indicates that neutrophil-delivered NE can act as a stimulatory factor in a variety of cancer types and serve as an independent prognostic indicator in patients with cancer of breast, lung, prostate, and colon (Akizuki et al., 2007; Lerman and Hammes, 2018; Sato et al., 2006). NE expression also has been associated with enhanced tumorigenesis in various animal models (Gong et al., 2013; Houghton et al., 2010; Lerman et al., 2017). NE is regarded as one of the modulators of tumorigenesis because its genetic deletion or pharmacological inhibition reduces tumor burden in some preclinical studies of solid cancer and leukemia (Lerman and Hammes, 2018).

As one of the potent pre-activated proteases, NE manifests somewhat broad substrate specificity in vitro, but NE activity appears to be functionally under-explored for in vivo conditions involving low physiological concentrations of the enzyme. Elevated levels of NE allow for digestion of not only elastin but also other extracellular matrix proteins, including laminin (Albrengues et al., 2018), and a number of transmembrane proteins, such as E-cadherin, VCAM-1, JAM-C, and G-CSF receptor (Colom et al., 2015; Levesque et al., 2001; Mayerle et al., 2005). NE also was shown to cleave and activate several cytokines, such as interleukin-1 (IL-1), granulocyte colony-stimulating factor (G-CSF), and vascular endothelial growth factor (VEGF) (Henry et al., 2016; Hunter et al., 2003; Kurtagic et al., 2009). A specific NE inhibitor Sivelestat suppressed growth of human tumor cells and their invasion, thereby reproducing effects of antibody-mediated neutrophil depletion in xenotransplantation (Ho et al., 2014; Lerman et al., 2017; Wada et al., 2006). However, the molecular mechanisms underlying the role of NE in inflammation-linked cancers remain poorly understood, especially with regard to tumor cell dissemination in the context of primary tumor microenvironment and specific stages of metastasis.

The goal of this study was to investigate where and when during cancer progression does NE activity assist tumor cells in their spread from the primary tumor to metastatic sites and what are the possible mechanisms involved in such assistance. Herein, we have demonstrated that at low pathophysiological concentrations, exogenously delivered NE was able to substantially enhance the levels of tumor cell intravasation, one of the earliest steps of cancer metastasis and quite distinct from the invasion step (Deryugina and Kiosses, 2017). Specifically, low picomole levels of NE induced tumor angiogenesis and enhanced entry of escaping primary tumor cells into a distinct set of dilated intratumoral angiogenic vessels capable of supporting intravasation. By employing NE knockout (KO) mice, we also have shown that after intravasation, NE enabled the vascular-arrested tumor cells to efficiently resist clearance and survive in secondary tissue sites. These key in vivo findings were further supported by our demonstration that NE induced Src/PI3K-dependent Akt signaling, mechanistically underlying the functional role of NE in early steps of cancer dissemination. Together with documentation of reduced tumor cell tissue retention and diminished spontaneous metastasis in NE-deficient hosts, this study strongly implicates NE as a potential translational target.

RESULTS

NE Is Involved in Tumor Cell Metastasis

To investigate the role of NE in early events of cancer cell dissemination, we employed a modification of the well-established chorioallantoic membrane (CAM) model of tumor cell intravasation and metastasis (Kim et al., 1998; Quigley and Armstrong, 1998), allowing for precise localized treatments of primary tumors (Deryugina, 2016). A human epidermoid carcinoma cell line, HEp3, representing an aggressive subset of head and neck cancer (Toolan, 1954), was the main source of tumor cells in these in vivo assays. On day 10 of embryo development, 1×10^5 HEp3 cells were grafted onto 6 separate areas of the CAM. Developing microtumors were treated daily with NE purified from human neutrophils. The delivery of IL-8, a potent neutrophil chemoattractant (Waugh and Wilson, 2008), was used as positive control to comparatively assess the effects of NE treatment. On day 5, portions of the liver were harvested and processed for quantification of disseminated tumor cells by human-specific Alu-qPCR.
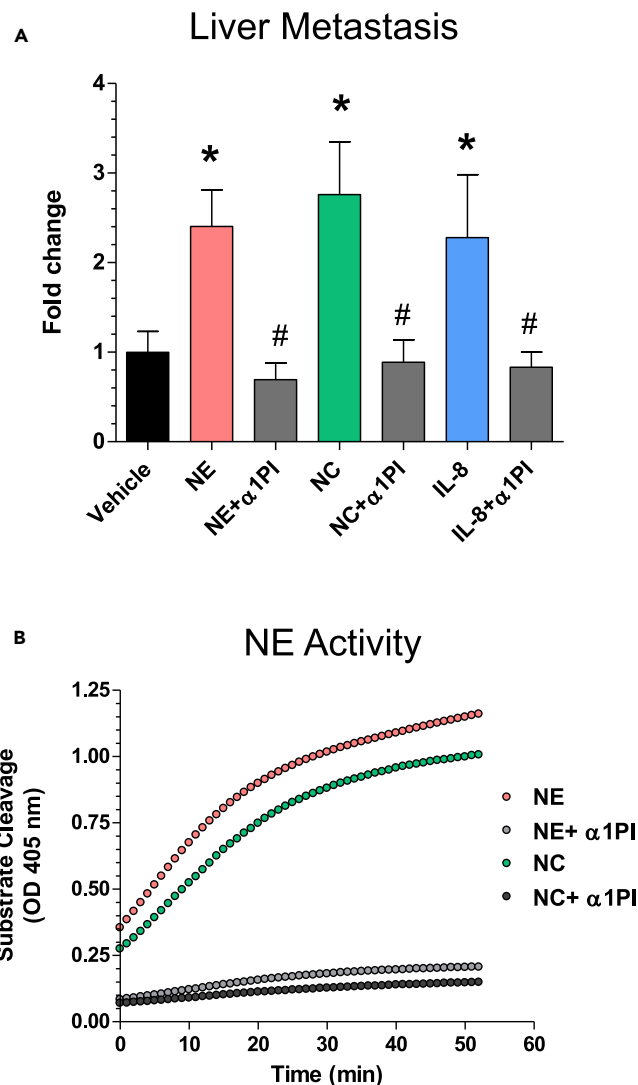
A

Liver Metastasis

B

NE Activity

Figure 1. NE Is Involved in Tumor Cell Metastasis

(A) Human HEp3 carcinoma cells were grafted onto the CAM of live, day 10 chick embryos (6 sites each containing 1×10^5 cells in 10 μL of native type I collagen at 2.3 mg/mL). Developing tumors were treated daily with topical applications of 10 μL solutions of PBS/1% DMSO, containing purified neutrophil elastase (NE) (100 nM), NE mixed with α1PI (0.3 μM), neutrophil cavitated (NC) preparations (100 nM of NE specific activity), NC mixed with α1PI (0.3 μM), IL-8 (100 ng), and IL-8 mixed with α1PI (0.3 μM). Control embryos were treated with vehicle solution (PBS/1% DMSO). On day 5, liver tissue was harvested, total DNA prepared and processed for human-specific *Alu*-qPCR to quantify the number of HEp3 cells within the chicken embryo background (10^6 cells). The data from individual experiments (5–7 embryos per variable) were normalized to the number of disseminated cells in the vehicle control group (fold differences), and the normalized data (up to 5 independent experiments) were combined for statistical assessment. *, p < 0.05 in Student's t test or Mann-Whitney U test compared with control. #, p < 0.05 in Student's t test or Mann-Whitney U-test compared with the corresponding group containing no α1PI. Data are presented as mean ± SEM.

(B) Inhibition of NE activity by α1PI. Enzymatic activity of NE and NC preparations was analyzed for the sensitivity to α1PI in a substrate cleavage assay. Purified human NE (100 nM) and NC (diluted 1:3 to achieve ~100 nM of NE activity), used alone or pre-mixed with 0.3 μM α1PI, were added to a 350 nM elastase-specific colorimetric substrate. Generation of the cleaved substrate was monitored for 60 min at 405 nM.

Daily treatments of HEp3 microtumors with exceptionally low levels of purified NE at 1 picomole/tumor (10 μL of 100 nM NE solution per tumor) significantly increased the levels of liver metastasis (Figure 1A). However, if NE was pre-mixed at a stoichiometric ratio of 1:3 with α1PI, this NE-specific serpin abrogated the metastasis-enhancing effect of NE (Figure 1A), coordinately inhibiting the enzyme's capacity to cleave an NE-specific substrate (Figure 1B).

Because NE is delivered predominantly, if not exclusively, by neutrophils releasing their secretory granules, we investigated whether neutrophil granule contents also would induce liver metastasis in an NE-activity-dependent manner. HEp3 tumors were treated with the total granule contents generated by nitrogen cavitation of purified neutrophils (Simpson, 2010). The neutrophil cavitates (NCs) were confirmed to be enzymatically potent in the NE-specific activity assay (Figure 1B) and delivered to HEp3 tumors at 1 picomole equivalent of active NE per microtumor (6 picomoles per embryo). Daily treatments with NCs significantly increased metastasis of HEp3 cells compared with vehicle-treated control (Figure 1A). Furthermore, α1PI substantially reduced the metastasis-inducing effect of NC and brought the levels of HEp3 cell metastasis to the vehicle control levels (Figure 1A; p < 0.04), indicating that native NE, contained within the total granule contents of human neutrophils, is capable of substantially facilitating cancer cell dissemination.

The metastasis-facilitating role of tumor-infiltrating neutrophils was further demonstrated by topical treatments of CAM tumors with IL-8, a potent tumor-cell-produced cytokine that attracts inflammatory neutrophils (Minder et al., 2015). The levels of HEp3 dissemination to the liver were significantly elevated by daily treatments of primary tumors with IL-8 (200 ng per tumor; p < 0.03). Importantly, a large percentage of IL-8-induced metastasis also was sensitive to α1PI (Figure 1A), again indicating NE as a metastasis-promoting, neutrophil-specific protease.

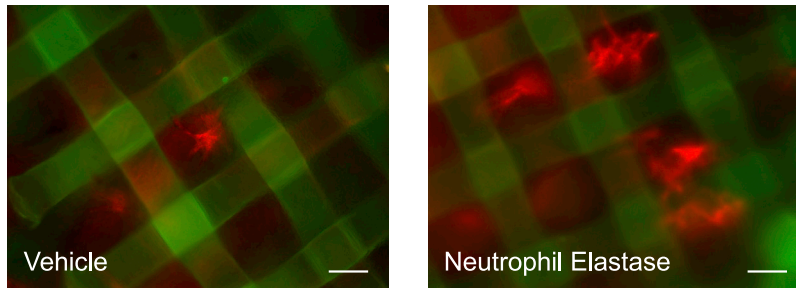### NE Affects Tumor Angiogenesis and Angiogenesis-Dependent Intravasation

We have recently shown that tumor cell intravasation occurs mainly within the developing tumor and involves *intratumoral* angiogenic blood vessels (Deryugina and Kiosses, 2017). This distinct subset of newly formed vasculature is represented by blood vessels with lumens of ~15–40 μm in diameter, which would readily accommodate the volume of intravasating tumor cell(s) (Minder et al., 2015). To investigate whether NE would aid in the development of these angiogenic vessels, we employed a collagen "on-plant" assay (Deryugina and Quigley, 2008), in which type I collagen rafts filled with GFP-tagged HEp3 cells were planted atop the CAM and treated daily with purified NE at low concentrations. After 3 days, the upward-sprouting, blood-carrying angiogenic vessels were counted between mesh grids of the collagen rafts, and the *angiogenic index* was calculated as the ratio of grids containing newly formed vessels versus total number of grids. Injection into embryos of the Rhodamine-conjugated lectin,LCA, resulted in red-fluorescent vessels visible against the grids of the onplant-supporting meshes (Figure 2A). Quantification indicated that NE treatment resulted in a 2-fold increase of the angiogenic index (p < 0.0001), consistent with NE functioning as a potent angiogenesis-inducing enzyme (Figure 2B). Portions of the CAM tissue distal to the collagen onplants were analyzed for the number of intravasated human HEp3 tumor cells. In tandem with the increased angiogenesis in these onplants, NE coordinately enhanced 2-fold the levels of HEp3 cell intravasation (Figure 2C; p < 0.05), indicating that at picomole levels, NE can induce the development of a functional angiogenic vasculature that provides conduits for the observed tumor cell dissemination.

NE Facilitates Development of a Dilated Intravasation-Sustaining Intratumoral Vasculature

To investigate how NE could affect the structure of an intratumoral vasculature, GFP-tagged HEp3 cells were grafted onto the CAM, and developing tumors were treated with purified NE delivered alone or in combination with α1PI. To probe NE effect on vessel structure and lumen diameter, tumor-bearing embryos were inoculated with Rhodamine-LCA to highlight the vasculature. Portions of the CAM containing treated or untreated primary tumors were excised, visualized under a fluorescence microscope, and the diameters of *intratumoral* blood vessels were measured across individual tumors (10–15 measurements per tumor). The percentages of vessels with diameters <15 μm, from 15 μm to 40 μm, and >40 μm were calculated for several independent experiments and combined for final statistical assessments.

Treatment with NE resulted in the development of intratumoral blood vessels having lumens larger than in control group, but not if NE was delivered along with α1PI (Figure 3A, first three panels from the left). Differential quantification indicated that blood vessels with lumens between 15 and 40 μm in diameter constituted less than 20% of all perfusable vessels in non-treated control tumors (Figure 3B, black bars). Purified NE induced a substantial, 2.7-fold increase in the fraction of the 15- to 40-μm vessels unless the proteolytic activity of NE was inhibited with α1PI (Figure 3B, red open and hatched bars). The low percentage of relatively large >40-μm vessels (4–8%) was not affected by any type of treatment (data not shown); however, the fraction of <15-μm vessels changed in a manner reciprocal to that of 15- to 40-μm vessels (Figure 3B, red
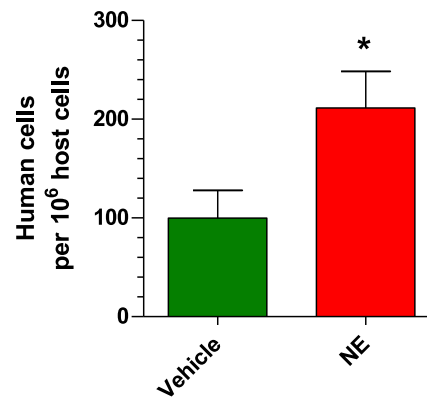
A Angiogenic vessels within collagen onplants

B Angiogenesis within collagen onplants
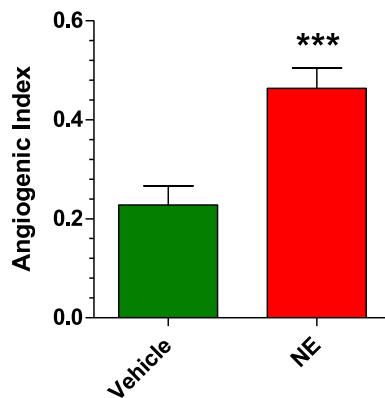
C HEp3 cell dissemination from collagen onplants

Figure 2. NE Affects Tumor Angiogenesis and Angiogenesis-Dependent Intravasation

(A) Grid rafts, each containing 30 μL of type I collagen (2.3 mg/mL) populated with GFP-tagged HEp3 cells (1×10^6/mL reconstituted collagen), were planted on the CAM of chick embryos. The "onplants" were treated on days 1 and 2 with purified neutrophil elastase (NE) (10 μL of 100 nM solution) or vehicle (PBS/1% DMSO). On day 3, the embryos were inoculated i.v. with red-fluorescent lectin, Rhodamine-conjugated LCA (100 μg in 0.1 mL PBS), to contrast blood vessels (red fluorescence) against the grids of onplant-supporting meshes. Scale bars, 100 μm.

(B) Angiogenic vessels containing visible circulating erythrocytes were counted between mesh grids of the collagen raft, and the angiogenic index was calculated as the ratio of grids containing newly formed functional blood vessels versus total number of grids. ***, $p < 0.05$ in Student's t test compared with the vehicle control. Data are presented as mean ± SEM.

(C) On day 5, the levels of HEp3 cell dissemination from the 3D collagen rafts were determined with human-specific *Alu*-qPCR in portions of CAM harvested far distal (1–5 cm) to the sites of onplant grafting. *, $p < 0.05$ in Student's t test compared with the vehicle control. Data are presented as mean ± SEM.

bars). Importantly, the increase in 15- to 40-μm vessels in the NE-treated group correlated well with a corresponding increase in tumor cell intravasation measured in the same tumor-bearing embryos (Figure 3C, red bars). These data indicate that NE induces the development of more dilated intratumoral blood vessels capable of sustaining tumor cell intravasation.

Similar approaches were employed in which HEp3 tumors were treated with NC preparations (Figure 3A, right two panels). Treatment with NC alone resulted in more than 3-fold increase in percentage of 15- to 40-μm vessels but not if NCs were supplemented with α1PI (Figure 3B, right set of blue bars, open versus hatched). In tandem with the induction of 15- to 40-μm vessels, NC preparations significantly induced the levels of HEp3 intravasation unless the α1PI serpin was present (Figure 3C, blue bars), again indicating that tumor-infiltrating neutrophils can deliver their active NE-containing granule contents to the sites of a primary tumor and induce an intravasation-supporting vasculature.
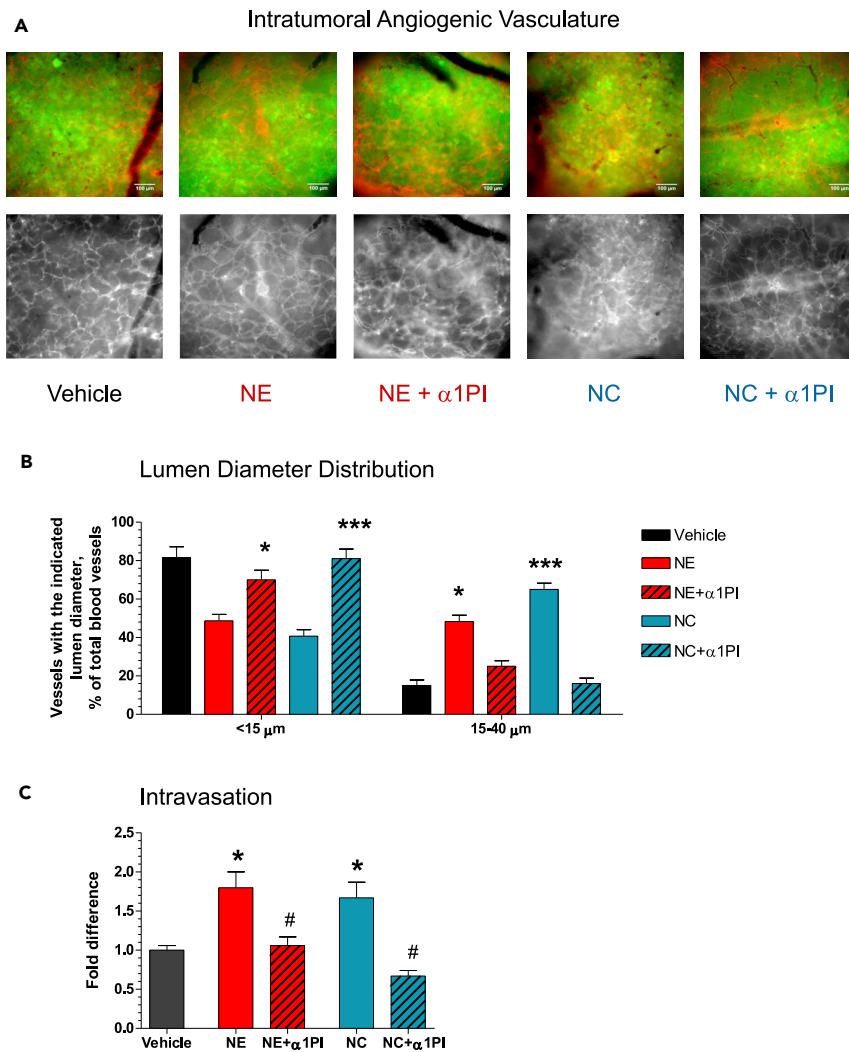
Figure 3. NE and Neutrophil Granule Content Facilitate the Development of an Intravasation-Sustaining Intratumoral Vasculature

(A) GFP-tagged HEp3 cells were grafted on the CAM and treated daily (10 μL per tumor, topical application) with vehicle (PBS/1% DMSO), purified neutrophil elastase (NE), alone (100 nM) or mixed with α1PI (0.3 μM), and neutrophil cavitated preparations (NC), alone (at 100 nM NE activity) or mixed with α1PI (0.3 μM). On day 5, the embryos were inoculated with Rhodamine-conjugated LCA (0.1 mL of 1 mg/mL solution in PBS) to contrast the intratumoral angiogenic vasculature against green fluorescence of human tumor cells. (*Top*) Tumor images with the signals of HEp3-GFP cells (green) and LCA-stained vessels (red) merged. Scale bars, 100 μm. (*Bottom*) Monochromatic images depicting intratumoral blood vessels only.

(B) The microtumors were analyzed for vessel diameter distribution on day 5 after cell grafting. Data are presented as mean ± SEM of at least 10 microtumors analyzed for each of control group and groups treated with NE (red bars) or NC (blue bars) with (hatched bars) or without (non-hatched, open bars) α1PI (from a total of 3 independent experiments). *, p < 0.05 in Student's t test compared with the vehicle control.

(C) Levels of intravasation were quantified by human-specific *Alu*-qPCR in the portions of the CAM harvested distal to primary tumors and presented as fold differences relative to vehicle control. Data are presented as mean ± SEM determined for three independent experiments involving from 7 to 38 embryos per variable. *, p < 0.05 in Student's t test compared with the vehicle control. #, p < 0.05 in Student's t test compared with the corresponding group containing no α1PI.

To substantiate the latter notion, tumor-bearing embryos were inoculated with freshly isolated human neutrophils (Figure 4). The delivery of viable, intact neutrophils induced a substantially dilated intratumoral vasculature unless their NE activity was blocked by α1PI (Figure 4A). Differential measurements
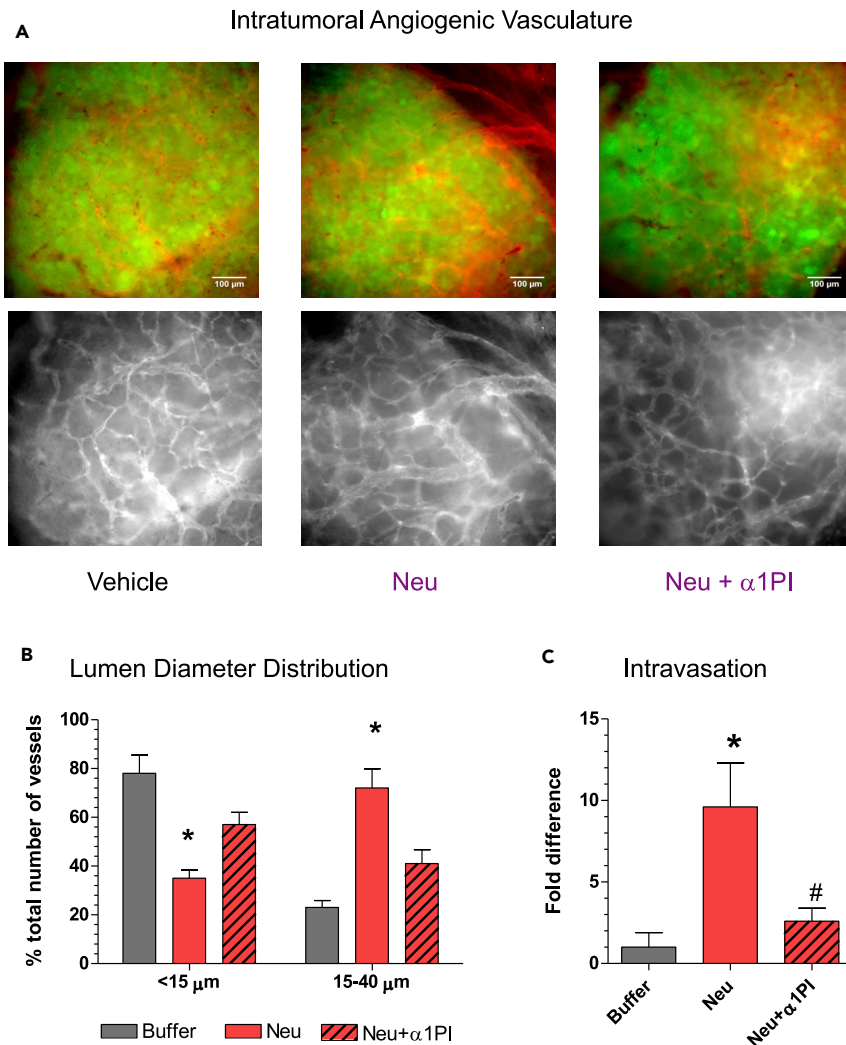
A Intratumoral Angiogenic Vasculature

Vehicle   Neu   Neu + α1PI

B Lumen Diameter Distribution

C Intravasation

Figure 4. Intact NE-Competent Neutrophils Facilitate the Development of Intravasation-Supporting Intratumoral Vasculature

(A) GFP-tagged HEp3 cells were grafted on the CAM within six 10-μL-collagen droplets, each containing 1×10^5 cells. On day 3, the embryos were inoculated with 2×10^6 neutrophils freshly isolated from human peripheral blood. In a set of embryos, the developing tumors were pre-treated with α1PI (0.3 μM) on day 1 and 2 and additionally treated after neutrophil inoculations on day 4. On day 5, the embryos were inoculated with Rhodamine-conjugated LCA (0.1 mL of 1 mg/mL solution in PBS) to contrast the intratumoral angiogenic vasculature against green fluorescence of human tumor cells. (*Top*) Representative IF images of tumors with signals for HEp3-GFP cells (green) and LCA-stained vessels (red) merged. Scale bars, 100 μm. (*Bottom*) Monochromatic images depicting intratumoral blood vessels only.

(B) The microtumors were analyzed for vessel diameter distribution on day 5 after cell grafting. Data are presented as mean ± SEM of at least 10 microtumors analyzed for each of control group and groups treated with neutrophils with or without α1PI (4 independent experiments). *, $p < 0.05$ in Student's t test compared with the vehicle control.

(C) On day 5 of tumor development, the numbers of human tumor cells within portions of the CAM distal to primary tumors were quantified by human-specific *Alu*-qPCR using a standard curve. The levels of intravasation are presented as fold differences relative to the buffer control. The data are mean ± SEM of four independent experiments involving a total of 24 embryos in the control group, 21 embryos in the group inoculated with neutrophils, and 6 embryos in the group treated with both neutrophils and α1PI. *, $p < 0.05$ in Student's t test compared with the vehicle control. #, $p < 0.05$ in Student's t test compared with the corresponding group containing no α1PI.

indicated that neutrophil treatments resulted in a 3-fold increase in 15- to 40-μm vessels (Figure 4B, red versus gray bars), along with a 5- to 10-fold increase in the levels of tumor cell intravasation (Figure 4C). However, when developing tumors were pre-treated with α1PI, neutrophil-mediated induction of 15- to
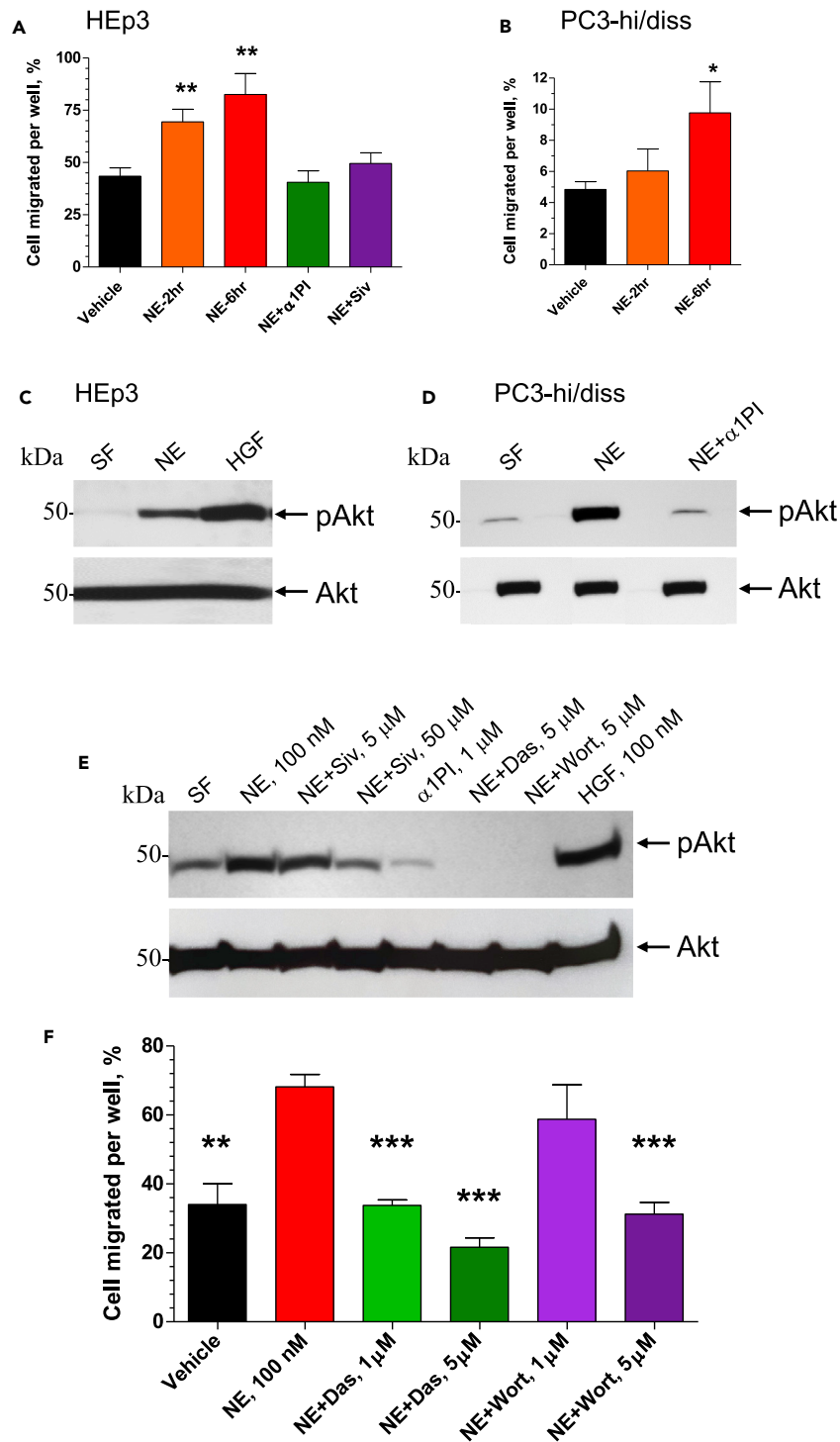
Figure 5. NE Induces Tumor Cell Migration via Src/PI3K-Dependent Akt Signaling

(A and B) Subconfluent cultures of HEp3 cells (A) and PC3-hi/diss cells (B) were pre-treated with 100 nM purified NE for 2 or 6 h and then washed twice in serum-free (SF) medium. NE inhibitors α1PI (1 μM) and Sivelestat (Siv; 50 μM) were added along with 100 nM NE to HEp3 cells for the 6-h incubation (A). Vehicle-treated cells (negative control) and NE-treated cells were placed into Transwell inserts (1 × 10⁵) and allowed to migrate toward chemoattractants in lower chamber (5% FCS). After 18- to 24-h incubation, the percentage of cells transmigrated into the lower chamber was quantified. From 2 to 3

Figure 5. *Continued*

experiments were performed for both cell types, each experiment in triplicate. * and **, p < 0.05 and p < 0.01, respectively, compared with vehicle control; two-tailed Student's t test. Data are presented as mean ± SEM.

(C and D) Serum-starved HEp3 (C) and PC3-hi/diss (D) cells were pre-treated for 20 min with purified NE (100 nM), alone or along with a1PI (1 mM), or hepatocyte growth factor (HGF; 50 nM), washed and lysed. Western blot analysis was performed on equal protein content (20 μg) under reducing conditions using antibodies against phosphorylated Akt (pAkt; upper panels) and total Akt (lower panels).

(E) Serum-starved HEp3 cells were pre-treated for 20 min with the NE inhibitor Sivelestat (5 μM or 50 μM) and α1PI (1 μM) or signaling inhibitors Dasatinib (Das, 5 μM) and Wortmannin (5 μM). Then, NE or HGF were added, both at 100 nM. After 20 min incubation, the cells were washed and lysed. Western blot analysis was performed on equal protein content (40 μg) under reducing conditions using antibodies against phosphorylated Akt (pAkt). Equal protein loading is indicated by the blot re-probed with antibodies against total Akt protein (Akt).

(F) HEp3 cells were pretreated for 6 h with vehicle or NE (100 nM), alone or mixed with Src inhibitor Dasatinib (Das; 1 μM or 5 μM) or PI3K inhibitor Wortmannin (Wort, 1 μM or 5 μM). Vehicle-treated cells (negative control) and NE-treated cells were placed into Transwell inserts (1×10^5) and allowed to migrate toward 5% FCS in the lower chamber. After 18- to 24-h incubation, the percentage of cells transmigrated into the lower chamber was quantified. ** and ***, p < 0.01 and p < 0.001, respectively, in comparison to the treatment with NE alone; two-tailed Student's t test.

Data are presented as mean ± SEM. See also Figures S1–S3.

40-μm vessels and tumor cell intravasation were both reduced to near control levels (Figures 4B and 4C).

Together, these findings strongly indicate that native NE activity released by inflammatory neutrophils infiltrating primary tumors greatly facilitates the early events of tumor cell dissemination, namely intratumoral angiogenesis, blood vessel dilation, and angiogenesis-dependent intravasation.

NE Induces Tumor Cell Migration via Src/PI3K-Dependent Akt Signaling

We investigated putative mechanisms and pathways, which could underlie the involvement of NE in tumor cell dissemination. Because primary tumor cells should exhibit enhanced migratory capabilities to separate from each other and actively enter the intratumoral angiogenic vessels during intravasation, we examined the effects of purified NE on efficiency of tumor cell migration. In addition to HEp3 epidermoid carcinoma cells, human prostate carcinoma PC3-hi/diss cells (Conn et al., 2009) were employed in this series of experiments.

The effects of NE on tumor cell migration were analyzed in Transwell assays in which tumor cells were pre-treated with 100 nM NE for 2 or 6 h, washed, placed into the upper chambers of Transwells, and allowed to transmigrate toward chemotactic stimuli. Pretreatment with active NE resulted in a time-dependent increase of migration rates for both HEp3 and PC3-hi/diss cells (Figures 5A and 5B). Pre-incubation with NE did not affect the growth rate of HEp3 and PC3-hi/diss cells within 2 days following treatment (Figure S1), eliminating proliferation-driven increase in the number of transmigrated cells from NE-mediated effects on tumor cell migration. However, NE-induced migration of HEp3 cells was completely abrogated by the NE inhibitor α1PI added at 1 μM (Figure 5A), indicating that the enzymatic activity of NE was required for stimulation of cell migration. This finding was further verified with the use of a synthetic NE inhibitor Sivelestat. Initially, the effectiveness of this low molecular weight inhibitor was evaluated in NE-mediated cleavage of cell surface CD44, demonstrating effectiveness of Sivelestat in a range of 3–10 μM concentrations (Figure S2). When applied to HEp3 cultures during NE treatment, Sivelestat diminished NE-induced cell migration, although it required 50 μM concentration of Sivelestat to be effective in contrast to 1 μM of α1PI (Figure 5A).

Tumor cells have to survive in circulation after the intravasation step and also in tissues after vascular arrest. Our previous studies on the proteolytic mechanisms elicited by neutrophil MMP-9, uPA, and plasmin during angiogenesis-dependent intravasation pointed to EGFR and Src/PI3K/Akt pathways as critically important for tumor cell migration toward, along, and inside the angiogenic vessels and early metastasis in our animal models (Casar et al., 2012, 2014; Deryugina and Kiosses, 2017; Minder et al., 2015). In this study we investigated in detail whether NE treatment would induce the activation of Akt, a critical member of survival and migration signaling pathways that previously was linked to cancer progression (Altomare and Testa, 2005). HEp3 and PC3-hi/diss cells were treated with 100 nM NE for 20 min and levels of Akt phosphorylation were measured in relation to the corresponding levels of total Akt. As shown in Figures 5C and 5D, Akt activation was induced by NE in HEp3 epidermoid carcinoma as well as PC3-hi/diss prostate carcinoma cells, indicating that NE can stimulate both the survival and motility of aggressive human cancer cells in Akt-dependent manner. In both cell types, NE-mediated induction of Akt activation was sensitive to 1 μM α1PI (Figures 5D and 5E), pointing out that the enzymatic activity

of NE is required for its cell-signaling-inducing effects. This effect of the natural NE inhibitor was reproduced by the synthetic inhibitor Sivelestat, however, at a 50 μM concentration (Figure 5E).

To investigate whether Src/PI3K pathway was involved in NE-induced Akt activation, we used the known Src inhibitor Dasatinib and PI3K inhibitor Wortmannin (Figure 5E). Before activation with NE, HEp3 cells were pre-treated for 20 min with 5 μM Dasatinib or Wortmannin and then treated with 100 nM NE for additional 20 min. Both inhibitors completely abrogated NE-induced Akt activation (Figure 5E). Together with the inhibition of NE-induced pathway activation by the NE inhibitors, α1PI and Sivelestat, these data indicate that Src and PI3K signaling pathways are involved in Akt activation induced by the enzymatic activity of NE (Figures 5C–5E).

We also probed for the role of mitogen-activated protein kinases (MAPKs) in NE-mediated effects on tumor cell migration, namely for the Erk1/2 and p38 MAPK pathways. Serum-starved HEp3 carcinoma cells were treated with NE or LPS used as a positive control for induction of phosphorylation of p38 and p42/p44. However, probing cell lysates for activation of p38 or p42/p44 did not indicate an involvement of p38 and Erk1/2 MAPK pathways in NE-induced responses of human HEp3 carcinoma cells used in the study (Figure S3).

We next examined whether the Src/PI3K/Akt pathway was involved in NE-induced cell migration by employing signaling inhibitors in Transwell assays (Figure 5F). Dasatinib completely abrogated the NE-induced portion of HEp3 cell migration when used at 1 μM, and - brought the migration levels below the vehicle control baseline when used at 5 μM (Figure 5F). Although Wortmannin at 1 μM did not significantly decrease cell migration, it efficiently inhibited it to the baseline level when used at 5 μM (Figure 5F). We also probed for the involvement of EGFR pathway, but an effective EGFR inhibitor Erlotinib did not reduce NE-increased cell migration even when used at 30 μM, indicating that EGFR activation apparently is not involved in NE-mediated signaling effects (data not shown).

Overall, these data provide evidence for the specificity of proteolytic effects of NE on cell migration as well as indicate that NE-mediated induction of tumor cell migration involves the Src/PI3K/Akt cell survival/signaling pathway.

NE Contributes to Vascular Arrest and Tissue Retention of Human Carcinoma Cells

The availability of NE-KO mice allowed us to directly investigate the role of NE in metastasis stages that follow tumor cell intravasation, namely vascular arrest and tissue retention. We employed our lung retention model in which human tumor cells are inoculated into genetically modified mice and their wild-type (WT) counterparts and then quantified by human-specific *Alu*-qPCR at defined time periods (Deryugina and Quigley, 2012). Minutes after tail vein injections, the majority of inoculated cells are arrested in the pulmonary vasculature. Within the following 14 h, a great majority (>85%) of the initially arrested cells is cleared (Figure 6A), while the remaining cells, retained in the lung tissue, represent the portion of survived cells that have a high potential to establish lung metastases. Because initial clearance of human tumor cells occurs long before any species-specific immune responses are triggered within the murine recipients, the ratio of tissue-retained over initially arrested cells (retention index) reflects the capability of the injected tumor cells to withstand vascular clearance independent of host adaptive immunity.

We initially compared whether the numbers of vascular-arrested human tumor cells were similar in mice of different genotypes, namely immunodeficient NOD-SCID BALB/c and WT C57BL/6 strains. The genetic and immunological background of the recipients did not affect the numbers of initially arrested cells nor did the presence or absence of NE in C57BL/6 mice (Figures 6A and 6B). However, the genetically enforced lack of NE was associated with a substantially reduced number of HEp3 cells retained within the lung tissue in NE-KO recipients compared with WT counterparts (Figures 6A and 6B). Correspondingly, the retention index for HEp3 cells in NE-KO mice dropped to 25% of that in NE-competent NOD-SCID and C57BL/6 WT mice (Figure 6C). Similar data were also obtained with human PC3-hi/diss prostate carcinoma cells. Although arrest in the lung vasculature was not affected by the lack of NE expression in NE-KO mice, injection of PC3-hi/diss cells into NE-KO mice resulted in significantly reduced percentage of retained cells as compared with WT recipients and reflected in a 65%–70% reduced retention index (Figure S4).

The close correspondence of the differential retentions between the microscopically visible fluorescent tumor cells and *Alu*-qPCR-quantified tumor cells (Figure 6 and S4) further validated our use of human-specific *Alu*-qPCR as a quantitative throughput analysis for tissue retention of vascular-arrested human tumor cells.
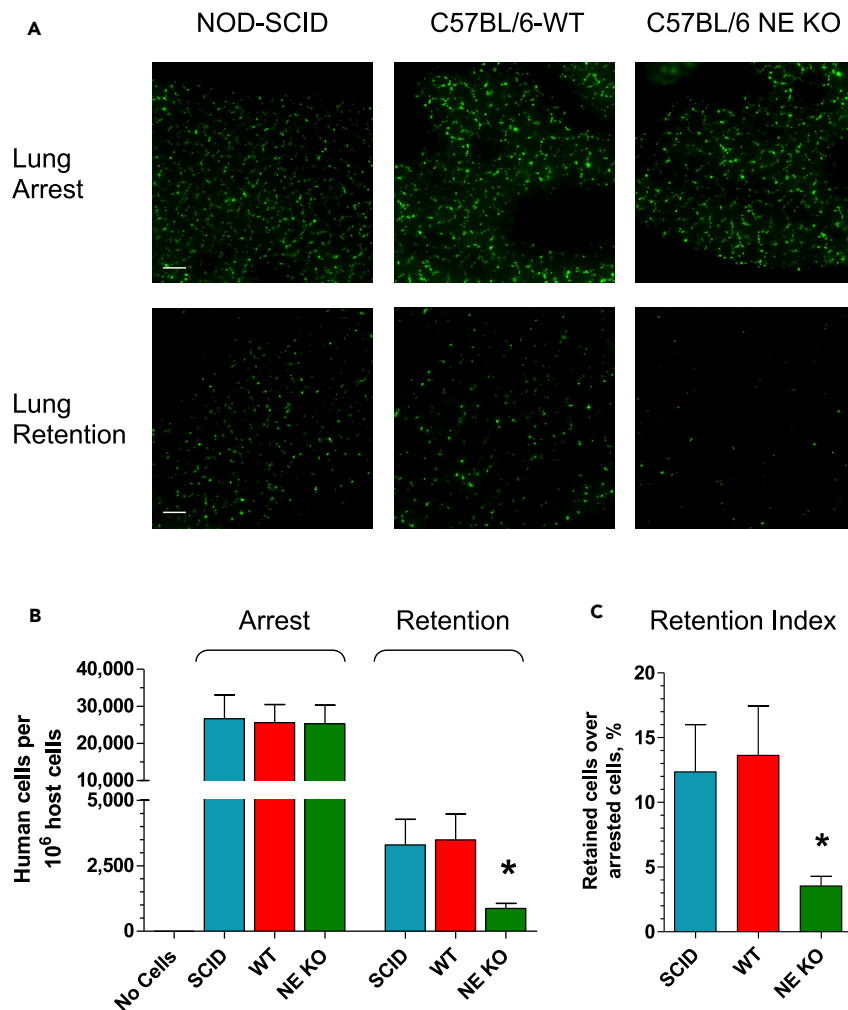
Figure 6. NE Contributes to Vascular Arrest and Tissue Retention of Human Carcinoma Cells

(A) GFP-tagged HEp3 cells were inoculated into the tail vein of immunodeficient SCID mice or C57BL/6 mice, WT type or NE-KO (5×10^5 cells per mouse). The lungs were excised 20 min or 14 h later to determine the levels of tumor cell arrest in the lung vasculature or tissue retention of vascular arrested cells, respectively. Green fluorescent HEp3 cells were imaged in the lungs at original 200× magnification in an immunofluorescence microscope equipped with a digital video camera. Scale bars, 100 μm.

(B) The number of inoculated HEp3 cells arrested and retained in the lung vasculature was measured in the lung tissue with human-specific *Alu*-qPCR. The lung tissue of mice that received no human tumor cells was used as negative control. Three independent experiments were performed involving a total of 14–17 mice per variable. *, $p < 0.05$, unpaired two-tailed Student's t test. Data are presented as mean ± SEM.

(C) Retention indices were quantified for each mouse as the percentage of HEp3 cells retained in the lung compared with the number of cells arrested in the lung vasculature, based on human-specific *Alu*-qPCR analyses. *, $p < 0.01$, unpaired two-tailed Student's t test.

Data are presented as mean ± SEM. See also Figures S4 and S5.

Overall these data document that host NE is important for retention of vascular-arrested tumor cells of different tissue origin and is independent of adaptive immunity but clearly dependent on an enzyme derived from an innate immune cell, namely the neutrophil.

NE Is Critical for Spontaneous Metastasis in a Syngeneic Mouse Model of Head and Neck Cancer

To corroborate our HEp3 carcinoma data from the avian model of spontaneous metastasis (Figures 1A, 3C and 4C), we employed murine oral carcinoma cells, MOC2, in syngeneic WT and NE-KO C57BL/6 mice in our
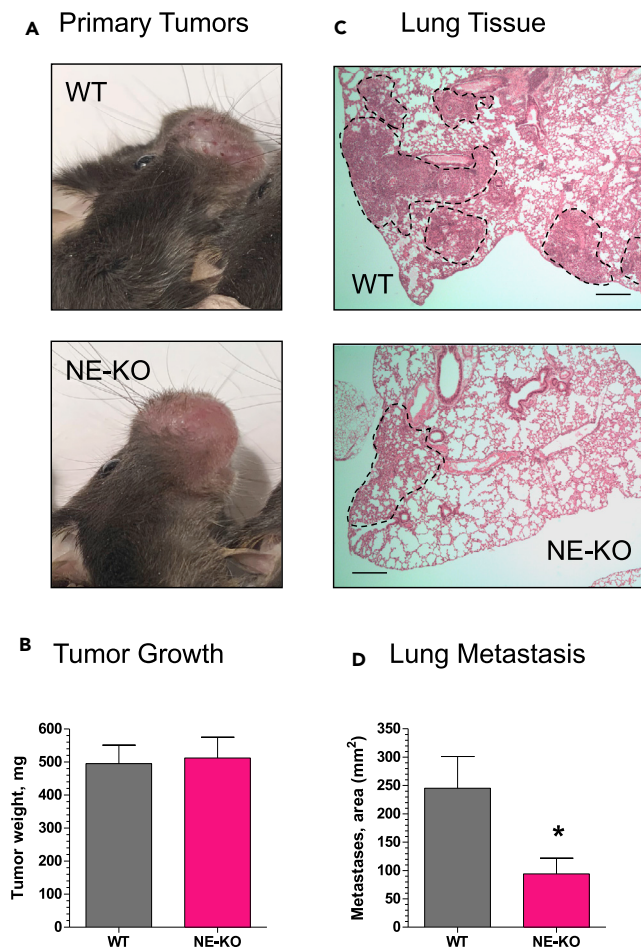
A Primary Tumors

C Lung Tissue

B Tumor Growth

D Lung Metastasis

Figure 7. NE Is Critical for Spontaneous Metastasis in a Syngeneic Mouse Model of Head and Neck Cancer

Murine head and neck cancer carcinoma cells, MOC2, were inoculated into the buccal mucosa of syngeneic WT or NE-KO C57BL/6 mice at 1×10^6 cells per site. Twelve to 14 days later (A), the mice were sacrificed and their primary buccal tumors weighed (B). The lungs were excised, fixed, and processed for staining with H&E (C). Scale bars, 1 mm. The areas of lung parenchyma filled with tumor cells (C, areas indicated by dashed lines) were quantified for each mouse against total area of lung tissue and expressed as "Metastases" area (D). Two independent experiments were performed, involving a total of 16 WT and 12 NE-KO mice. *, $p < 0.05$; unpaired two-tailed Student's t test. The numerical data are presented as mean $\pm$ SEM.

orthotopic model of head and neck cancer metastasis (Deryugina et al., 2018). In this model, the oral squamous carcinoma cells are inoculated into the buccal mucosa of the upper lip and after primary tumors reach ~1 cm in diameter, the mice are sacrificed and their lung tissue is examined for metastasis, lungs being the major meta-static site in human head and neck cancer (Daiko et al., 2010). In preliminary experiments we noted that the over-all tumor growth was slightly impaired in NE-KO mice, therefore 30% more MOC2 cells were implanted into these recipients (1.3×10^6 cells/site) compared to their WT counterparts (1×10^6 cells per site). This approach allows for the changes in lung metastasis to be attributed to the ability of tumor cells to disseminate in different genetic environments rather than to the differences in primary tumor size.

Primary MOC2 tumors reached ~500 mg 12 days after cell inoculations into buccal mucosa, and the tumors developed in WT and NE-KO mice were overall similar in gross appearance (Figure 7A) and weight (Figure 7B). However, staining of lung sections indicated that metastatic MOC2 cells occupied considerably more interstitial spaces between the lung alveoli in WT mice compared to NE-KO recipients (Figure 7C). Quantification indicated that there was a significant ~70% reduction of lung metastasis in the mice lacking NE (Figure 7D), clearly indicating a functional role for NE during spontaneous metastasis of cancer cells disseminating from orthotopic primary tumors in a syngeneic mammalian model system.

DISCUSSION

Substantial evidence exists linking neutrophil influx into developing tumors with cancer progression and subsequent metastatic dissemination (Coffelt et al., 2016; Fridlender and Albelda, 2012; Liang and Ferrara, 2016; Nicolas-Avila et al., 2017; Powell and Huttenlocher, 2016; Uribe-Querol and Rosales, 2015). The evidence has come from various *in vivo* models, employing exogenously added neutrophil populations or investigating tumor-recruited endogenous neutrophils, and from cancer patient data showing high neutrophil-lymphocyte ratio in blood and elevated tumor-associated neutrophils (TANs) in biopsies and resections (Fridlender and Albelda, 2012; Peng et al., 2015). Multiple reasons have been offered to account for heightened tumor progression with a coordinately enhanced neutrophil influx. The evidence-based reasons stem from conventional observations that inflammatory neutrophils, driven by tumor-derived chemokines, are first responders on the scene, and biochemical demonstrations that the release of neutrophil products, including hyperoxides and oxidases, cytokines and chemokines, and peptides and proteases, can stimulate immune responses, angiogenesis, NETosis, specific signaling pathways, and increased tumor cell migration, invasion, and dissemination (Albrengues et al., 2018; Papayannopoulos et al., 2010; Powell and Huttenlocher, 2016).

The quantitative *in vitro* and *in vivo* data presented herein imply that NE, a potent serine protease, should be considered as a major inflammatory neutrophil product that directly modulates tumor cell behavior, tumor-host interactions, and critical initial steps in the metastatic cascade. Supporting this conclusion are the data generated in our *in vivo* model systems, where we employed human and murine carcinoma cells in two host species (avian and murine) to examine *early* metastatic events, including angiogenesis, development of dilated neovasculature, tumor cell intravasation, lung tissue retention of tumor cells, and initial spread of intravasated cells. Concurrently and coordinately with the levels of tumor cell intravasation and metastasis, the presence or absence of active NE differentially altered the vascularity, structure of host-tumor tissue, and extent of tumor cell dissemination.

NE levels in our animal models were manipulated via attraction of endogenous tumor-infiltrating neutrophils with neutrophil-specific chemoattractant agents (e.g., IL-8) or by exogenous delivery of total granule cavitates or purified active NE. Importantly, NE was supplemented at picomole levels of active enzyme per tumor per day, yet these exceptionally low levels resulted in a 2- to 8-fold change in tumor angiogenesis (Figure 2), carcinoma cell intravasation (Figures 3 and 4), and liver metastasis (Figure 1). To our knowledge, these effects have not been reported before, and our observed differentials *in vivo* indicate that NE is one of the most potent natural effector molecules/enzymes delivered by host neutrophils influxing the tumor milieu.

The specific removal of NE activity in the animal models initially was achieved by employing the natural NE inhibitor, α1PI. This serpin, the most abundant serine proteinase inhibitor in plasma, exhibits a potent inhibitory capacity against neutrophil serine proteases, particularly NE (Janciauskiene et al., 2018). Two other neutrophil proteases, proteinase 3 and cathepsin G, can also be inhibited by α1PI but at concentrations more than 10-fold higher than needed for NE inhibition, and therefore α1PI is considered as primarily acting to inhibit NE (Janciauskiene et al., 2018; Korkmaz et al., 2010). As shown in Figure 1B, α1PI effectively inhibited activity of 100 nM NE when used at stoichiometric level of 0.3 μM. When supplemented at a concentration of 1 μM, α1PI was also very effective in the inhibition of NE-induced Akt activation (Figures 5D and 5E). Furthermore, inhibition of NE proteolytic activity by added α1PI caused a coordinated reduction of the effects elicited by exogenous NE on intravasation of HEp3 carcinoma cells (Figures 3 and 4). These *in vivo* data are consistent with a previously reported pharmacological inhibition of lung cancer through the upregulation of α1PI (Xu et al., 2012).

To strengthen the case for requirement of the proteolytic activity for NE-induced effects, we used the low-molecular-weight, synthetic NE inhibitor Sivelestat in some of our *in vitro* and *in vivo* experiments. We demonstrated that at 3–10 μM concentration, Sivelestat efficiently prevented proteolytic activity of NE (Figure S2). However, a 50 μM concentration of Sivelestat was required to efficiently reduce NE-induced Akt activation and cell migration compared to a 1 μM concentration- of α1PI (Figure 5). These data confirm relative inefficiency of this inhibitor in cell function assays in other studies demonstrating that 10–200 μM concentrations of Sivelestat were required to significantly inhibit NE-induced responses in tumor cells *in vitro* (Aikawaa et al., 2011; Kumagai et al., 2013; Lerman et al., 2017; Okeke et al., 2020; Wada et al., 2006). Overall, our findings show that two distinct NE inhibitors, the native α1PI and the synthetic Sivelestat, can block NE-induced cell migration, requiring NE enzymatic activity and NE-mediated Akt activation, both critical for enhanced cell motility and survival.

We also explored the putative inhibitory effects of Sivelestat *in vivo*. In agreement with the relatively low efficacy of Sivelestat in cell function assays *in vitro*, the inhibitor failed to significantly reduce tumor cell

numbers in the lung retention model *in vivo*, even when it was used via i.p. or i.v. routes, at a dose 1–2 mg/mouse (50–100 mg/kg), and injected up to 3 times within 12- to 14-h duration of the lung retention assay (Figure S5). These findings are consistent with several published studies indicating the poor pharmacokinetics of Sivelestat and requirement for its daily, repetitive or continuous infusions in animal models (Aikawaa et al., 2011; Kumagai et al., 2013; Lerman et al., 2017; Okeke et al., 2020; Wada et al., 2006). In general, our *in vivo* Sivelestat data are in line with the overall inefficiency of low-molecular-weight synthetic protease inhibitors, including NE inhibitors, in reducing metastases in cancer animal models and clinical trials (Fields, 2019; Okeke et al., 2020), in part due to their rapid *in vivo* clearance, off target effects, and/or timing of administration.

An alternative removal of NE was achieved via genetic elimination of NE in NE-KO (*Elane*$^{-/-}$) mice, which were employed in our animal model systems designed to assess the metastatic events subsequent to intravasation, namely vascular arrest and lung retention (Figure 6 and S4). Another model, where the absence of NE was genetically enforced, involved metastasis of murine oral carcinoma cells from buccal primary tumors to secondary lung tissue, the preferred metastatic site of oral squamous cell carcinomas (Figure 7). In both cases, the absence of NE in NE-KO host neutrophils substantially reduced the specific tissue retention of vascular-arrested human oral and prostate carcinoma cells in a xenogeneic experimental metastasis model, as well as the dissemination of murine oral carcinoma cells in an orthotopic syngeneic metastasis model. These results provide additional evidence that host NE, delivered to early stage tumors by first-responding innate immune cells, is an essential effector molecule for ensuing cancer metastasis.

Other reports have demonstrated that NE-KO mice exhibit significant phenotypic changes compared to WT mice, including reduced emphysema (Shapiro et al., 2003), reduced fibrosis (Gregory et al., 2015), and diminished tumor cell proliferation in primary tumors and secondary growths (Houghton et al., 2010), all demonstrating involvement of NE in these pathological processes. Uniquely adding to this evidence, our NE-KO data and our *in vivo* NE addition-inhibition experiments indicate that NE is critical for certain events in the metastatic cascade, namely intravasation of escaping primary tumor cells and retention/survival of disseminating tumor cells in the lung vascular network.

An additional aspect of NE related to metastatic dissemination was its effect on tumor angiogenesis and structure-function aspects of the newly formed neovasculature. Purified NE, supplemented daily to HEp3 tumor cell-CAM onplants at only 1–2 picomoles, caused a significant 2-fold increase in the angiogenic index, and interestingly, the same NE-treated tumor onplants yielded a 2-fold increase in tumor cell intravasation (Figure 2). Quantitative measurements of lumen diameters in the intratumoral vasculature demonstrated a 2- to 3-fold increase in the fraction of dilated vessels in the NE-treated tumors (Figure 3). Nearly identical results were obtained regardless whether NE-mediated effects were mediated by purified enzyme, crude neutrophil cavitates, or intact viable neutrophils, suggesting that the dilated neovessels represented those angiogenic conduits that sustained NE-mediated increase in tumor cell intravasation. Noteworthy, a long-term connection has been established between larger diameters of microvessels in primary tumors with enhanced metastatic disease in cancer patients (Sugino et al., 2002; Yamamura et al., 2001), further supporting the importance of tumor-associated vessel diameter in the intravasation step that precedes metastasis (Chiang et al., 2016).

In order to further interrogate possible mechanisms underlying the pleiotropic effects of host NE on the tumor vasculature, several *in vitro* studies were conducted. We showed that NE enhanced the chemotactic migratory capacity of HEp3 and PC3-hi/diss tumor cells, providing a possible explanation for the escape and active entry of these primary tumor cells into the intratumoral vasculature. We also demonstrated that NE stimulated the activation of Akt, a critical component of intracellular survival pathway signaling, and showed that NE-induced Akt activation was sensitive to NE inhibitors, α1PI and Sivelestat, and cell signaling inhibitors, the Src inhibitor Dasatinib and the PI3K inhibitor Wortmannin. These *in vitro* results provide a plausible NE/Akt-mediated mechanism for the NE-enhanced cell survival and tissue retention exhibited by tumor cells following intravasation. A number of intracellular signaling pathways have been linked to NE-mediated activation of transmembrane proteins or release of membrane bound ligands (Lerman and Hammes, 2018). In addition, one report indicates that NE can cross into tumor cells, activate the Akt pathway, and enhance lung tumor growth via degradation of the intracellular insulin receptor substrate-1 (Houghton et al., 2010). Thus, multiple extracellular and intracellular mechanisms may operate downstream of NE catalytic activity, but until now NE has not been definitively associated as functionally

involved with specific early steps in metastasis. Previously we demonstrated that divergent signaling pathways can be elicited in metastasizing cancer cells in response to different proteases such as MMP-1, MMP-9, or plasmin (Casar et al., 2012, 2014; Juncker-Jensen et al., 2013; Minder et al., 2015). Furthermore, we showed that diverse signaling pathways can be induced by the same protease, e.g., PARP1 and FAK/PI3K/Akt signaling in response to plasmin (Casar et al., 2012; Casar et al., 2014) or FGFR and EGFR signaling in response to MMP-9 (Ardi et al., 2009; Minder et al., 2015)). Our documented EGFR signaling elicited by neutrophil MMP-9 (Minder et al., 2015) and Src/PI3K/Akt signaling elicited by NE shown in the present study indicate that distinct signaling responses can be induced by specific proteases originating from the same cell source, namely inflammatory neutrophils.

An inherent implication of our overall results is that NE released by responding neutrophils is catalytically operating in at least two distinct early stages of metastatic dissemination. One stage appears to be at the juncture of a growing tumor and its newly forming *intratumoral* vasculature. Active NE, naturally released or exogenously added, is affecting the development and lumen structure of the intratumoral blood vessels, thereby facilitating primary tumor cell intravasation. This action of NE may be continuous or additive over the period of neutrophil influx and also dependent on enzyme stabilization in the tissue. The second stage, where NE appears to function, is indicated by the lack-of-function data from NE-KO murine models (Figures 6, 7 and S4). In NE-competent hosts, this step of cancer cell dissemination would involve NE acting on the vascular arrested tumor cells within the capillary network of a secondary site. At this particular stage, the NE released by neutrophils responding to vascular-arrested tumor cells would act directly within the tumor-vascular microenvironment and enable disseminating cancer cells to avoid a massive clearance, to survive, and be retained in the tissue. Our data indicate 2- to 3-fold higher levels of lung retention for human tumor cells in WT versus NE-KO mice. A possible explanation for this NE-dependent clearance avoidance and tissue retention stems from results showing that purified NE induces the Src/PI3K-dependent Akt survival signaling pathway in two metastatic human carcinoma cell types employed in the present study. The catalytic activity of NE exerted at two distinct stages would imply that different cell types, i.e. vascular endothelial cells and/or vascular arrested tumor cells, and different protein substrates could be the targets of NE action. Thus far, with the exception of CD44, we have not identified *bona fide* NE-specific target substrates, the cleavage of which might yield some of the pronounced structural and functional changes we documented *in vivo*. Proteomic and molecular-genetic approaches should aid in the identification of functional NE substrates within or on the surface of aggressive tumor cells and facilitate the demonstration that NE-mediated cleavage of identified targets is directly causal to the NE-mediated processes we have uncovered in this study.

It can be translattionallty challenging to further demonstrate that *intrinsic* NE enhances tumor cell dissemination in cancer patients. A few chemical inhibitors of NE have shown limited success in clinical trials for treatment of non-cancerous disorders of the lung (Aikawa and Kawasaki, 2014; von Nussbaum and Li, 2015); however, clinical trials employing highly specific NE inhibitors for cancer patients have not yet been reported. The critical interactions of human tumor cells with NE documented herein might be readily targetable because the metastasis-enhancing action of NE appears to operate in the extracellular milieu of the engaged tumor tissue following influx of inflammatory neutrophils. The activity of NE also appears to function within the targetable intratumoral neovasculature in response to vascular-arrested tumor cells at a putative secondary site. The latter notion is consistent with the studies, which demonstrated a metastasis-promoting engagement of neutrophils in experimental metastasis (Labelle and Hynes, 2012) or during tumor-induced preparation of metastatic niches for the arrival of disseminating primary tumor cells (Kaplan et al., 2006). However, neither of these studies identified the specific neutrophil product that was causal for enhancing metastasis. Our findings indicate that both the delivery by inflammatory neutrophils of their NE and the extracellular NE activity itself might be pharmacologically targeted shortly after diagnosis of early tumor development. According to NE-KO studies, the normal physiological role of NE is quite mild or not apparent unless challenged by infection, injury, or tumor growth (Gong et al., 2013; Kessenbrock et al., 2008; Kolaczkowska et al., 2009). Therefore, molecular neutralization of NE might not be as deleterious for cancer patients as pharmacologically induced systemic neutropenia, further supporting a translational targeting of heightened NE activity locally, within the cancerous microenvironment. This notion might especially be considered in those particular precancerous situations, where the chronic influx of inflammatory neutrophils and delivery of their NE might be widespread.

Limitations of the Study

In this study we investigated the functional contribution of NE to early stages of metastasis. The major experimental approaches involved the supplementation of developing tumors with exogenous NE and

the use of NE-KO mice. However, we were not able to demonstrate the effectiveness of systemic inhibition of intrinsic NE with a small molecule inhibitor Sivelestat. An additional limitation is related to the lack of mouse model in which NE expression could be switched off specifically in the neutrophils. This mouse model would have allowed us to demonstrate tumor-promoting activity of NE delivered distinctively by inflammatory neutrophils during different phases of primary tumor growth and primary tumor cell dissemination. We also demonstrated that NE-mediated activation of Src/PI3K/Akt pathway was critical for survival and migration of tumor cells and excluded EGFR and MAPK pathways as activated by NE in our models. However, it is possible that other pathways could be activated by NE and important for tumor cell metastasis.

Resource Availability

Lead Contact

Further requests should be directed to and will be fulfilled by the Lead Contact: Elena Deryugina (deryugin@scripps.edu).

Materials Availability

No new unique reagents were generated in this study.

Data and Code Availability

No unpublished custom code, software, algorithm, or datasets were used in this study.

METHODS

All methods can be found in the accompanying Transparent Methods supplemental file.

SUPPLEMENTAL INFORMATION

Supplemental Information can be found online at https://doi.org/10.1016/j.isci.2020.101799.

ACKNOWLEDGMENTS

AUTHOR CONTRIBUTIONS

J.P.Q and E.D. conceived and designed the project. E.D., A.C., V.A., T.M., and J.S. performed and analyzed experiments. C.P. was involved in supervising NE-KO studies and helped in editing manuscript. J.P.Q. and E.D. wrote the manuscript.

DECLARATION OF INTERESTS

The authors declare no competing interests.

REFERENCES

Aikawa, N., and Kawasaki, Y. (2014). Clinical utility of the neutrophil elastase inhibitor sivelestat for the treatment of acute respiratory distress syndrome. Ther. Clin. Risk Manag. *10*, 621–629.

Aikawaa, N., Ishizaka, A., Hirasawa, H., Shimazaki, S., Yamamoto, Y., Sugimoto, H., Shinozaki, M., Taenaka, N., Endo, S., Ikeda, T., et al. (2011). Reevaluation of the efficacy and safety of the neutrophil elastase inhibitor, Sivelestat, for the treatment of acute lung injury associated with systemic inflammatory response syndrome; a

phase IV study. Pulm. Pharmacol. Ther. *24*, 549–554.

Akizuki, M., Fukutomi, T., Takasugi, M., Takahashi, S., Sato, T., Harao, M., Mizumoto, T., and Yamashita, J. (2007). Prognostic significance of immunoreactive neutrophil elastase in human breast cancer: long-term follow-up results in 313 patients. Neoplasia *9*, 260–264.

Albrengues, J., Shields, M.A., Ng, D., Park, C.G., Ambrico, A., Poindexter, M.E., Upadhyay, P.,

Uyeminami, D.L., Pommier, A., Kuttner, V., et al. (2018). Neutrophil extracellular traps produced during inflammation awaken dormant cancer cells in mice. Science *361*, eaao4227.

Altomare, D.A., and Testa, J.R. (2005). Perturbations of the AKT signaling pathway in human cancer. Oncogene *24*, 7455–7464.

Ardi, V.C., Kupriyanova, T.A., Deryugina, E.I., and Quigley, J.P. (2007). Human neutrophils uniquely release TIMP-free MMP-9 to provide a potent

catalytic stimulator of angiogenesis. Proc. Natl. Acad. Sci. U. S. A. *104*, 20262–20267.

Ardi, V.C., Van den Steen, P.E., Opdenakker, G., Schweighofer, B., Deryugina, E.I., and Quigley, J.P. (2009). Neutrophil MMP-9 proenzyme, unencumbered by TIMP-1, undergoes efficient activation in vivo and catalytically induces angiogenesis via a basic fibroblast growth factor (FGF-2)/FGFR-2 pathway. J. Biol. Chem. *284*, 25854–25866.

Casar, B., He, Y., Iconomou, M., Hooper, J.D., Quigley, J.P., and Deryugina, E.I. (2012). Blocking of CDCP1 cleavage in vivo prevents Akt-dependent survival and inhibits metastatic colonization through PARP1-mediated apoptosis of cancer cells. Oncogene *31*, 3924–3938.

Casar, B., Rimann, I., Kato, H., Shattil, S.J., Quigley, J.P., and Deryugina, E.I. (2014). In vivo cleaved CDCP1 promotes early tumor dissemination via complexing with activated beta1 integrin and induction of FAK/PI3K/Akt motility signaling. Oncogene *33*, 255–268.

Chantrain, C.F., Shimada, H., Jodele, S., Groshen, S., Ye, W., Shalinsky, D.R., Werb, Z., Coussens, L.M., and DeClerck, Y.A. (2004). Stromal matrix metalloproteinase-9 regulates the vascular architecture in neuroblastoma by promoting pericyte recruitment. Cancer Res. *64*, 1675–1686.

Chiang, S.P., Cabrera, R.M., and Segall, J.E. (2016). Tumor cell intravasation. Am. J. Physiol. Cell Physiol. *311*, C1–C14.

Coffelt, S.B., Wellenstein, M.D., and de Visser, K.E. (2016). Neutrophils in cancer: neutral no more. Nat. Rev. Cancer *16*, 431–446.

Colom, B., Bodkin, J.V., Beyrau, M., Woodfin, A., Ody, C., Rourke, C., Chavakis, T., Brohi, K., Imhof, B.A., and Nourshargh, S. (2015). Leukotriene B4-neutrophil elastase axis drives neutrophil reverse transendothelial cell migration in vivo. Immunity *42*, 1075–1086.

Conn, E.M., Botkjaer, K.A., Kupriyanova, T.A., Andreasen, P.A., Deryugina, E.I., and Quigley, J.P. (2009). Comparative analysis of metastasis variants derived from human prostate carcinoma cells: roles in intravasation of VEGF-mediated angiogenesis and uPA-mediated invasion. Am. J. Pathol. *175*, 1638–1652.

Crusz, S.M., and Balkwill, F.R. (2015). Inflammation and cancer: advances and new agents. Nat. Rev. Clin. Oncol. *12*, 584–596.

Daiko, H., Nagai, K., Yoshida, J., Nishimura, M., Hishida, T., Ebihara, M., Miyazaki, M., Shinozaki, T., Miyamoto, S., Sakuraba, M., et al. (2010). The role of pulmonary resection in metastatic tumors from head and neck carcinomas. Jpn. J. Clin. Oncol. *40*, 639–644.

Deryugina, E.I. (2016). Chorioallantoic membrane microtumor model to study the mechanisms of tumor angiogenesis, vascular permeability, and tumor cell intravasation. Methods Mol. Biol. *1430*, 283–298.

Deryugina, E.I., and Kiosses, W.B. (2017). Intratumoral cancer cell intravasation can occur independent of invasion into the adjacent stroma. Cell Rep. *19*, 601–616.

Deryugina, E.I., and Quigley, J.P. (2008). Chapter 2. Chick embryo chorioallantoic membrane models to quantify angiogenesis induced by inflammatory and tumor cells or purified effector molecules. Methods Enzymol. *444*, 21–41.

Deryugina, E.I., and Quigley, J.P. (2012). Cell surface remodeling by plasmin: a new function for an old enzyme. J. Biomed. Biotechnol. *2012*, 564259.

Deryugina, E.I., Zajac, E., Zilberberg, L., Muramatsu, T., Joshi, G., Dabovic, B., Rifkin, D., and Quigley, J.P. (2018). LTBP3 promotes early metastatic events during cancer cell dissemination. Oncogene *37*, 1815–1829.

Dongre, A., and Weinberg, R.A. (2019). New insights into the mechanisms of epithelial-mesenchymal transition and implications for cancer. Nat. Rev. Mol. Cell Biol. *20*, 69–84.

Fields, G.B. (2019). The rebirth of matrix metalloproteinase inhibitors: moving beyond the dogma. Cells *8*, 984.

Fridlender, Z.G., and Albelda, S.M. (2012). Tumor-associated neutrophils: friend or foe? Carcinogenesis *33*, 949–955.

Gong, L., Cumpian, A.M., Caetano, M.S., Ochoa, C.E., De la Garza, M.M., Lapid, D.J., Mirabolfathinejad, S.G., Dickey, B.F., Zhou, Q., and Moghaddam, S.J. (2013). Promoting effect of neutrophils on lung tumorigenesis is mediated by CXCR2 and neutrophil elastase. Mol. Cancer *12*, 154.

Gonzalez, H., Robles, I., and Werb, Z. (2018). Innate and acquired immune surveillance in the postdissemination phase of metastasis. FEBS J. *285*, 654–664.

Gregory, A.D., Kliment, C.R., Metz, H.E., Kim, K.-H., Kargl, J., Agostini, B.A., Crum, L.T., Oczypok, E.A., Oury, T.A., and Houghton, A.M. (2015). Neutrophil elastase promotes myofibroblast differentiation in lung fibrosis. J. Leukoc. Biol. *98*, 143–152.

Henry, C.M., Sullivan, G.P., Clancy, D.M., Afonina, I.S., Kulms, D., and Martin, S.J. (2016). Neutrophil-derived proteases escalate inflammation through activation of IL-36 family cytokines. Cell Rep. *14*, 708–722.

Ho, A.-S., Chen, C.-H., Cheng, C.-C., Wang, C.-C., Lin, H.-C., Luo, T.-Y., Lien, G.-S., and Chang, J. (2014). Neutrophil elastase as a diagnostic marker and therapeutic target in colorectal cancers. Oncotarget *5*, 473–480.

Houghton, A.M., Rzymkiewicz, D.M., Ji, H., Gregory, A.D., Egea, E.E., Metz, H.E., Stolz, D.B., Land, S.R., Marconcini, L.A., Kliment, C.R., et al. (2010). Neutrophil elastase-mediated degradation of IRS-1 accelerates lung tumor growth. Nat. Med. *16*, 219–223.

Huh, S.J., Liang, S., Sharma, A., Dong, C., and Robertson, G.P. (2010). Transiently entrapped circulating tumor cells interact with neutrophils to facilitate lung metastasis development. Cancer Res. *70*, 6071–6082.

Hunter, M.G., Druhan, L.J., Massullo, P.R., and Avalos, B.R. (2003). Proteolytic cleavage of granulocyte colony-stimulating factor and its receptor by neutrophil elastase induces growth

inhibition and decreased cell surface expression of the granulocyte colony-stimulating factor receptor. Am. J. Hematol. *74*, 149–155.

Janciauskiene, S., Wrenger, S., Immenschuh, S., Olejinicka, B., Greulich, T., Welte, T., and Chorostowska-Wynimko, J. (2018). The multifaceted effects of alpha1-antitrypsin on neutrophil functions. Front. Pharmacol. *9*, Article 341.

Jodele, S., Blavier, L., Yoon, J.M., and DeClerck, Y.A. (2006). Modifying the soil to affect the seed: role of stromal-derived matrix metalloproteinases in cancer progression. Cancer Metastasis Rev. *25*, 35–43.

Jodele, S., Chantrain, C.F., Blavier, L., Lutzko, C., Crooks, G.M., Shimada, H., Coussens, L.M., and Declerck, Y.A. (2005). The contribution of bone marrow-derived cells to the tumor vasculature in neuroblastoma is matrix metalloproteinase-9 dependent. Cancer Res. *65*, 3200–3208.

Juncker-Jensen, A., Deryugina, E.I., Rimann, I., Zajac, E., Kupriyanova, T.A., Engelholm, L.H., and Quigley, J.P. (2013). Tumor MMP-1 activates endothelial PAR1 to facilitate vascular intravasation and metastatic dissemination. Cancer Res. *73*, 4196–4211.

Kaplan, R.N., Rafii, S., and Lyden, D. (2006). Preparing the "soil": the premetastatic niche. Cancer Res. *66*, 11089–11093.

Kessenbrock, K., Frohlich, L., Sixt, M., Lammermann, T., Pfister, H., Bateman, A., Belaaouaj, A., Ring, J., Ollert, M., Fassler, R., et al. (2008). Proteinase 3 and neutrophil elastase enhance inflammation in mice by inactivating antiinflammatory progranulin. J. Clin. Invest. *118*, 2438–2447.

Kessenbrock, K., Plaks, V., and Werb, Z. (2010). Matrix metalloproteinases: regulators of the tumor microenvironment. Cell *141*, 52–67.

Kettritz, R. (2016). Neutral serine proteases of neutrophils. Immunol. Rev. *273*, 232–248.

Kim, J., Yu, W., Kovalski, K., and Ossowski, L. (1998). Requirement for specific proteases in cancer cell intravasation as revealed by a novel semiquantitative PCR-based assay. Cell *94*, 353–362.

Kolaczkowska, E., Grzybek, W., van Rooijen, N., Piccard, H., Plytycz, B., Arnold, B., and Opdenakker, G. (2009). Neutrophil elastase activity compensates for a genetic lack of matrix metalloproteinase-9 (MMP-9) in leukocyte infiltration in a model of experimental peritonitis. J. Leukoc. Biol. *85*, 374–381.

Korkmaz, B., Horwitz, M.S., Jenne, D.E., and Gauthier, F. (2010). Neutrophil elastase, proteinase 3, and cathepsin G as therapeutic targets in human diseases. Pharmacol. Rev. *62*, 726–759.

Kumagai, K., Saikawa, Y., Takeguchi, H., Suda, K., Fukuda, K., Nakamura, R., Takahashi, T., Kawakubo, H., Wada, N., Miyasho, T., et al. (2013). The neutrophil elastase inhibitor sivelestat suppresses accelerated gastrointestinal tumor growth via peritonitis after cecal ligation and puncture. Anticancer Res. *33*, 3653–3660.

Kurtagic, E., Jedrychowski, M.P., and Nugent, M.A. (2009). Neutrophil elastase cleaves VEGF to generate a VEGF fragment with altered activity. Am. J. Physiol. Lung Cell. Mol. Physiol. 296, L534–L546.

Labelle, M., and Hynes, R.O. (2012). The initial hours of metastasis: the importance of cooperative host-tumor cell interactions during hematogenous dissemination. Cancer Discov. 2, 1091–1099.

Lerman, I., Garcia-Hernandez, M.d.l.L., Rangel-Moreno, J., Chiriboga, L., Pan, C., Nastiuk, K.L., Krolewski, J.J., Sen, A., and Hammes, S.R. (2017). Infiltrating myeloid cells exert protumorigenic actions via neutrophil elastase. Mol. Cancer Res. 15, 1138–1152.

Lerman, I., and Hammes, S.R. (2018). Neutrophil elastase in the tumor microenvironment. Steroids 133, 96–101.

Levesque, J.P., Takamatsu, Y., Nilsson, S.K., Haylock, D.N., and Simmons, P.J. (2001). Vascular cell adhesion molecule-1 (CD106) is cleaved by neutrophil proteases in the bone marrow following hematopoietic progenitor cell mobilization by granulocyte colony-stimulating factor. Blood 98, 1289–1297.

Liang, W., and Ferrara, N. (2016). The complex role of neutrophils in tumor angiogenesis and metastasis. Cancer Immunol. Res. 4, 83–91.

Mantovani, A., Cassatella, M.A., Costantini, C., and Jaillon, S. (2011). Neutrophils in the activation and regulation of innate and adaptive immunity. Nat. Rev. Immunol. 11, 519–531.

Marvel, D., and Gabrilovich, D.I. (2015). Myeloid-derived suppressor cells in the tumor microenvironment: expect the unexpected. J. Clin. Invest. 125, 3356–3364.

Mayerle, J., Schnekenburger, J., Kruger, B., Kellermann, J., Ruthenburger, M., Weiss, F.U., Nalli, A., Domschke, W., and Lerch, M.M. (2005). Extracellular cleavage of E-cadherin by leukocyte elastase during acute experimental pancreatitis in rats. Gastroenterology 129, 1251–1267.

Minder, P., Zajac, E., Quigley, J.P., and Deryugina, E.I. (2015). EGFR regulates the development and microarchitecture of intratumoral angiogenic vasculature capable of sustaining cancer cell intravasation. Neoplasia 17, 634–649.

Mocsai, A. (2013). Diverse novel functions of neutrophils in immunity, inflammation, and beyond. J. Exp. Med. 210, 1283–1299.

Nicolas-Avila, J.A., Adrover, J.M., and Hidalgo, A. (2017). Neutrophils in homeostasis, immunity, and cancer. Immunity 46, 15–28.

Nozawa, H., Chiu, C., and Hanahan, D. (2006). Infiltrating neutrophils mediate the initial angiogenic switch in a mouse model of multistage carcinogenesis. Proc. Natl. Acad. Sci. U S A 103, 12493–12498.

Okeke, E., Louttit, C., Fry, C., Najafabadi, A.H., Han, K., Nemzek, J., and Moon, J. (2020). Inhibition of neutrophil elastase prevents neutrophil extracellular trap formation and rescues mice from endotoxic shock. Biomaterials 238, Article 119836.

Opdenakker, G., Van den Steen, P.E., Dubois, B., Nelissen, I., Van Coillie, E., Masure, S., Proost, P., and Van Damme, J. (2001). Gelatinase B functions as regulator and effector in leukocyte biology. J. Leukoc. Biol. 69, 851–859.

Ouzounova, M., Lee, E., Piranlioglu, R., El Andaloussi, A., Kolhe, R., Demirci, M.F., Marasco, D., Asm, I., Chadli, A., Hassan, K.A., et al. (2017). Monocytic and granulocytic myeloid derived suppressor cells differentially regulate spatiotemporal tumour plasticity during metastatic cascade. Nat. Commun. 8, 14979.

Papayannopoulos, V., Metzler, K.D., Hakkim, A., and Zychlinsky, A. (2010). Neutrophil elastase and myeloperoxidase regulate the formation of neutrophil extracellular traps. J. Cell Biol. 191, 677–691.

Peng, B., Wang, Y.-H., Liu, Y.-M., and Ma, L.-X. (2015). Prognostic significance of the neutrophil to lymphocyte ratio in patients with non-small cell lung cancer: a systemic review and meta-analysis. Int. J. Clin. Exp. Med. 8, 3098–3106.

Pham, C.T. (2006). Neutrophil serine proteases: specific regulators of inflammation. Nat. Rev. Immunol. 6, 541–550.

Powell, R.M., and Huttenlocher, A. (2016). Neutrophils in the tumor microenvironment. Trends Immunol. 37, 41–52.

Quigley, J.P., and Armstrong, P.B. (1998). Tumor cell intravasation alu-cidated. The chick embryo opens the window. Cell 94, 281–284.

Sato, T., Takahashi, S., Mizumoto, T., Harao, M., Akizuki, M., Takasugi, M., Fukutomi, T., and Yamashita, J.-i. (2006). Neutrophil elastase and cancer. Surg. Oncol. 15, 217–222.

Shapiro, S.D., Goldstein, N.M., Houghton, A.M., Kobayashi, D.K., Kelley, D., and Belaaouaj, A. (2003). Neutrophil elastase contributes to cigarette smoke-induced emphysema in mice. Am. J. Pathol. 163, 2329–2335.

Shojaei, F., Singh, M., Thompson, J.D., and Ferrara, N. (2008). Role of Bv8 in neutrophil-dependent angiogenesis in a transgenic model of cancer progression. Proc. Natl. Acad. Sci. U S A 105, 2640–2645.

Simpson, R.J. (2010). Disruption of cultured cells by nitrogen cavitation. Cold Spring Harbor. Protoc. 2010, 5513.

Stapels, D.A.C., Geisbrecht, B.V., and Rooijakkers, S.H.M. (2015). Neutrophil serine proteases in antibacterial defense. Curr. Opin. Microbiol. 23, 42–48.

Strell, C., Lang, K., Niggemann, B., Zaenker, K.S., and Entschladen, F. (2010). Neutrophil granulocytes promote the migratory activity of MDA-MB-468 human breast carcinoma cells via ICAM-1. Exp. Cell Res. 316, 138–148.

Sugino, T., Kusakabe, T., Hoshi, N., Yamaguchi, T., Kawaguchi, T., Goodison, S., Sekimata, M., Homma, Y., and Suzuki, T. (2002). An invasion-independent pathway of blood-borne metastasis: a new murine mammary tumor model. Am. J. Pathol. 160, 1973–1980.

Tam, E.M., Morrison, C.J., Wu, Y.I., Stack, M.S., and Overall, C.M. (2004). Membrane protease proteomics: isotope-coded affinity tag MS identification of undescribed MT1-matrix metalloproteinase substrates. Proc. Natl. Acad. Sci. U S A 101, 6917–6922.

Taniguchi, K., and Karin, M. (2018). NF-kappaB, inflammation, immunity and cancer: coming of age. Nat. Rev. Immunol. 18, 309–324.

Toolan, H.W. (1954). Transplantable human neoplasms maintained in cortisone-treated laboratory animals: H.S. No. 1; H.Ep. No. 1; H.Ep. No. 2; H.Ep. No. 3; and H.Emb.Rh. No. 1. Cancer Res. 14, 660–666.

Uribe-Querol, E., and Rosales, C. (2015). Neutrophils in cancer: two sides of the same coin. J. Immunol. Res. 2015, 21.

von Nussbaum, F., and Li, V.M.J. (2015). Neutrophil elastase inhibitors for the treatment of (cardio)pulmonary diseases: into clinical testing with pre-adaptive pharmacophores. Bioorg. Med. Chem. Lett. 25, 4370–4381.

Wada, Y., Yoshida, K., Hihara, J., Konishi, K., Tanabe, K., Ukon, K., Taomoto, J., Suzuli, T., and Mizuiri, H. (2006). Sivelestat, a specific neutrophil elastase inhibitor, suppresses the growth of gastric carcinoma cells by preventing the release of transforming growth factor-α. Cancer Sci. 97, 1037–1043.

Waugh, D.J., and Wilson, C. (2008). The interleukin-8 pathway in cancer. Clin. Cancer Res. 14, 6735–6741.

Xu, Y., Zhang, J., Han, J., Pan, X., Cao, Y., Guo, H., Pan, Y., An, Y., and Li, X. (2012). Curcumin inhibits tumor proliferation induced by neutrophil elastase through the upregulation of α1-antitrypsin in lung cancer. Mol. Oncol. 6, 405–417.

Yamamura, T., Tsukikawa, S., Yamada, K., and Yamaguchi, S. (2001). Morphologic analysis of microvessels in colorectal tumors with respect to the formation of liver metastases. J. Surg. Oncol. 78, 259–264.

Zhou, J., Nefedova, Y., Lei, A., and Gabrilovich, D. (2018). Neutrophils and PMN-MDSC: their biological role and interaction with stromal cells. Semin. Immunol. 35, 19–28.

Supplemental Information

Neutrophil Elastase Facilitates

Tumor Cell Intravasation

and Early Metastatic Events

Elena Deryugina, Alexia Carré, Veronica Ardi, Tomoki Muramatsu, Jonas Schmidt, Christine Pham, and James P. Quigley
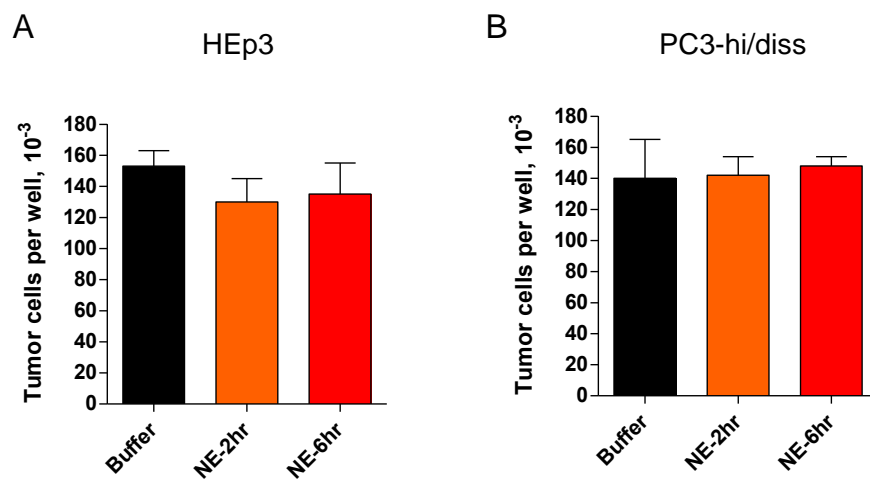
Supplemental Figures

Figure S1. NE does not affect tumor cell proliferation. Related to Figure 5.

HEp3 (**A**) and PC3-hi/diss (**B**) tumor cells were treated with 100 nM NE for 2 or 6 hr, washed and plated at $5x10^4$ cells per well in triplicate. After 48-hr incubation, the cells were detached and counted. Two independent experiments were performed for each tumor cell type. Data are presented as mean ± SEM.
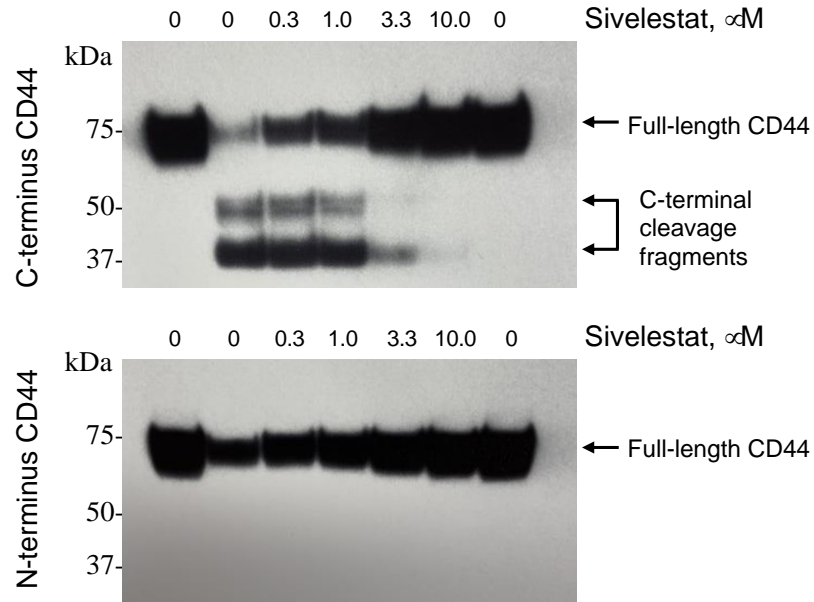
Figure S2. Inhibition of NE-mediated cleavage of CD44 by Sivelestat. Related to Figure 5.

PC3-hi/diss cells were left untreated or treated with 50 nM NE alone or pre-mixed with Sivelestat at the indicated increasing concentrations (0.3 to 10 mM). After 8-hr-incubation, the cell in each treatment culture (detached and still attached) were washed and lysed. Equal amounts of cell lysates (40 μg/lane) were probed under non-reducing conditions for the C-terminus and N-terminus CD44 with the corresponding terminus-specific antibodies. The blots indicate that CD44 is efficiently cleaved as evidenced by the diminishment of the extracellular N-terminal portion of 75 kDa full length CD44 and appearance of C-terminal cleavage fragments. At 3-10-μM range, Sivelestat efficiently blocked NE-mediated cleavage of CD44.
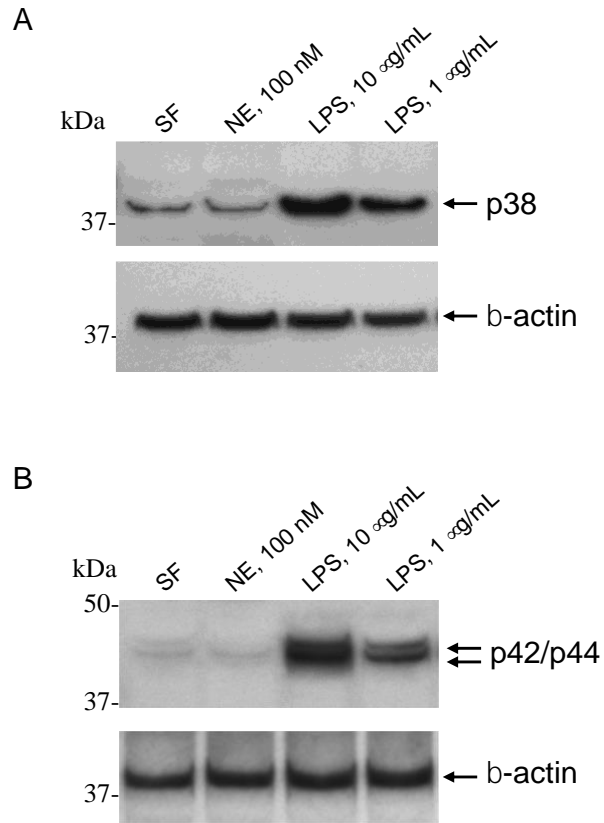
Figure S3. NE does not induce activation of p38 and Erk1/2 MAPKs. Related to Figure 5.

(**A**) HEp3 cells were serum starved and then treated with 100 nM NE for 20 min or 1 or 10 mg/ml LPS for 6 hours as a positive control for activation of p38 (**A**) or Erk1/2 (**B**). Equal amount of protein in cell lysates were loaded per lane (40 μg) of a gel run under reduced conditions. The phosphorylation of p38 and Erk1/2 was analyzed with the corresponding specific antibodies against phosphorylated p38 and p42/p44. Equal load was confirmed by probing blots for β-actin.
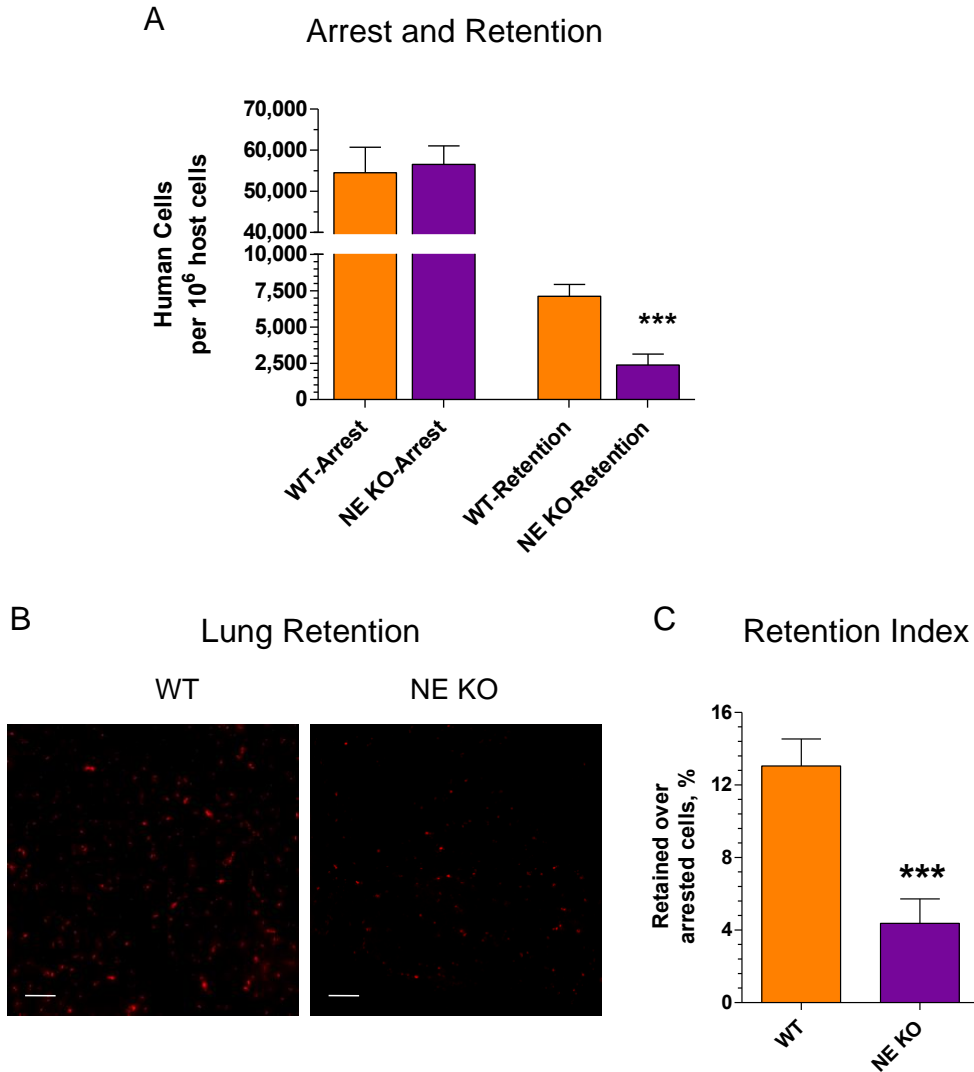
Figure S4. NE is required for efficient lung retention of vascular-arrested PC3-hi/diss cells. Related to Figure 6.

(**A**) PC3-hi/diss cells were stained with red-fluorescence dye (Abcam) and inoculated into the tail vein of C57BL/6 mice, WT or NE-KO (1×10^6 cells per mouse). The numbers of tumor cells arrested in the lung vasculature and cells retained in the lung tissue were measured within 20 min and 14 hr after cell inoculations, respectively, with human-specific *Alu*-qPCR. Two independent experiments were performed involving a total of 10 to 12 mice per variable. ***, $P<0.001$, two-tailed Student's *t*-test. Data are presented as mean ± SEM.

(**B**) Red-fluorescent PC3-hi/diss tumor cells were imaged in the lungs in an immunofluorescence microscope equipped with a digital video camera. Original magnification, 200x. Bar, 100 μm.

(**C**) Retention indices were quantified for each mouse as the fraction (%) of PC3-hi/diss cells retained in the lung compared to the number of inoculated cells initially arrested in the lung vasculature. ***, $P<0.01$, two-tailed Student's *t*-test. Data are presented as mean ± SEM.
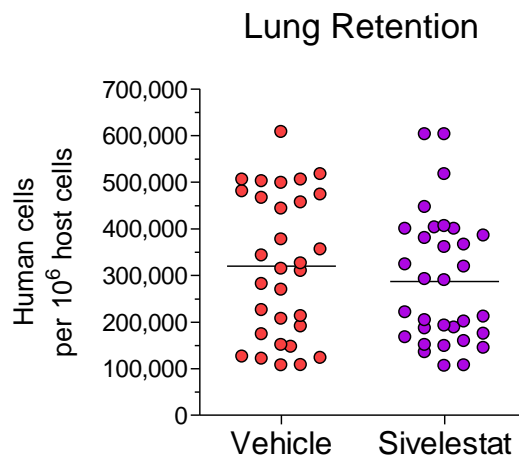
Figure S5. Lack of inhibitory effects of Sivelestat on lung retention. Related to Figure 6.

HEp3 cells were inoculated into the tail vein of immunodeficient SCID mice at $1x10^6$ cells per mouse. The mice were treated with a total of 1 to 3.5 mg Sivelestat per mouse, administered by i.p. or i.v. routes, 2-3 times within the 12 hr period before lung harvest. Control mice received equal volume of vehicle (4% DMSO in PBS). The number of HEp3 cells retained in the lung after 12 hr following cell inoculation was measured with human-specific *Alu*-qPCR. Four independent experiments involving a total of 30 and 31 mice per vehicle control and Sivelestat were performed. The individual mouse data from these experiments were pooled since there were no effects of Sivelestat regardless of the delivery route, number of inoculations, or dose.

Transparent Methods

Chemicals and reagents

Purified NE was purchased from Athens Research & Technology, Inc. (Athens, Georgia). Natural inhibitor α1PI and protease and phosphatase inhibitor cocktails were from Sigma (St Louis, MO). Synthetic NE inhibitor Sivelestat was from Cayman Chemical. Interleukin 8 (IL-8) was purchased from Peprotech (Rocky Hill, NJ). Antibodies against p38 MAPK phosphorylated at Thr180/Tyr182 (#9216) and p44/42 (Erk1/2) phosphorylated at Thr202/Tyr 204 (#9106). were from Cell Signaling.

Isolation of human neutrophils and preparation of nitrogen cavitates

Human neutrophils were isolated from whole blood obtained from healthy donors at the Scripps Research Institute. Two volumes of anti-coagulated blood (50mM EDTA) were layered over a double gradient formed by carefully layering one volume of Histopaque-1077 over one volume of Histopaque-1119 (both from Sigma-Aldrich). Blood cells were separated by centrifugation for 30 min at $700 \times g$. The upper plasma layer and mononuclear cells at the plasma/Histopaque-1077 interface were removed. The granulocytes were harvested from the Histopaque-1077/1119 interface and washed twice with cold Hanks Balanced Salt Solution (HBSS, Thermo Fisher Scientific) by centrifugation for 10 min at $400 \times g$. Washed granulocytes were re-suspended at the desired concentration in serum-free (SF) DMEM supplemented with gentamicin (10 µg/mL). The purity of neutrophil fraction was verified with HEMO staining (Protocol) and was >95%. To open granule contents, isolated neutrophils placed into the cryogenic tubes at $1x10^7$ cells/mL HBSS. Tubes were subjected to 3 freeze/thawing cycles in liquid nitrogen/warm water bath. After centrifugation at 4 min, $4000 \times g$, 4°C, the cell debris was removed and the nitrogen cavitates (NC) were kept at -20°C until use.

NE activity assay

To determine the NE activity in NC preparations, 30 µL of the sample were mixed with 350 nM of the elastase colorimetric substrate (Elastase substrate I, Calbiochem) in ammonium bicarbonate buffer (50 nM). The enzyme activity was assayed by a colorimetric detection at 405 nm (SynergyMX, BioTek) using a calibration curve generated by titration of purified NE. Kinetic assays were run for 1h, allowing for the determination of Vmax values and calculation of NE activity using the Gen5 2.0 software.

Tumor cells and culture conditions

Human epidermoid HEp3 carcinoma cell line (Toolan, 1954) and an aggressive variant of human PC3 prostate carcinoma cell line possessing high disseminating potential, PC3-hi/diss (Conn et al., 2009), were used in this study. Murine carcinoma cells, MOC2, generated to study head and neck cancer in syngeneic mouse models ((Judd et al., 2012), were received from Dr. R. Upalluri of Washington School of Medicine (St. Louis, MO). Cells were cultured in Dulbecco's modified Earle's medium (DMEM), supplemented with glucose, sodium pyruvate, non-essential amino acids, gentamycin and 10% FBS (D10). For using in experiments, the cells were detached with enzyme-free buffer, washed in serum-free (SF) DMEM, and re-suspended in desired concentration.

Cell proliferation and chemotactic cell migration

HEp3 and PC3 cells were treated with purified NE at 100 nM for 2 or 6 hours, washed and suspended at $1x10^6$ cells/mL SF-DMEM. For cell proliferation assays, washed cells were plated at $5x10^5$ per well of 24-well cluster in D10. After 48 hours, cells were detached with trypsin-EDTA and counted. For cell migration assays, washed cells were plated at $1x10^5$ per insert of a 6.5-µm Transwell with 8-µm pore size membrane. Cells were allowed to migrate towards chemoattractant in an outer chamber, 5% FBS or 100 nM of hepatocyte growth factor (HGF). Transmigrated cells were harvested after overnight incubation and counted. For NE inhibition experiments, the cells were first pretreated with NE inhibitors, α1PI and Sivelestat, or signaling inhibitors, Dasatinib and Wortmannin, at the indicated concentrations for 20 min, and then the cultures were treated with NE.

Western blotting

Sub-confluent layers of tumor cells plated the day before experiment were washed in SF-DMEM and treated with 100 nM purified NE for 20 min. For NE inhibition experiments, the cells were first pretreated with NE inhibitors, α1PI and Sivelestat or signaling inhibitors Dasatinib and Wortmannin at the indicated concentrations for 20 min, and then the cultures were treated with NE. Cells were lysed on ice with mRIPA buffer supplemented with the protease and phosphatase inhibitors (Sigma). Cell lysates were clarified by centrifugation and equal protein contents (20-40 µg/lane) were separated by SDS-PAGE on 4-20% gels. The separated proteins were transferred to a PVDF membrane, blocked with 1% BSA, and incubated overnight with the mouse monoclonal antibody against Akt, phospho Akt, phospo p38, phosphor Erk1/2, β-actin (all from Cell Signaling), C-terminal CD44 (Rb antibody from Boster), or N-terminal CD44 mouse mAb 29-7 generated in our laboratory. The membranes were washed and incubated with the secondary antibodies conjugated with HRP (Cell Signaling). The bound secondary antibodies were visualized with West Pico substrate (Thermo Fisher Scientific).

Animal studies

All experiments involving animals were conducted in accordance with the Animal Protocol approved by TSRI Animal Care and Use Committee (IACUC).

CAM angiogenesis model

The effects of purified NE on tumor cell-induced angiogenesis were determined using a collagen onplant angiogenesis assay as described (Deryugina and Quigley, 2008a). Briefly, GFP-tagged HEp3 cells were incorporated at $1x10^6$ cells per mL into 2.2 mg/mL neutralized native type I collagen (BD Biosciences) and 30 µL-droplets of the mixture were polymerized over grid meshes (3x4 mm) generating three-dimensional (3D) rafts ("onplants") by incubating at 37^0C for 20 min. Solidified onplants were grafted onto the chorioallantoic membrane (CAM) of 10 day-old chick embryos incubated *ex ovo* (6 onplants/embryo). The onplants were treated daily with 10 µL of 100 nM of NE or vehicle (PBS/1% DMSO). Within 68 h to 72 h, newly developed blood vessels that had grown into 3D collagen rafts were scored over the lower mesh using a stereoscope. The angiogenic index was calculated for each onplant as the ratio of number of grids having newly formed blood vessels over the total number of scored grids. To visualize the angiogenic blood vessels within collagen rafts, the onplant-bearing embryos were injected via

the allantoic vein with 100 ug of Rhodamine-conjugated *Lens culinaris* agglutinin (LCA; Vector laboratories) in 0.1 mL PBS. Portions of CAM with onplants were visualized for fluorescence in an Olympus microscope equipped with a digital video camera. To measure tumor cell intravasation, portions of CAM, 1-5 cm distal to collagen onplants, were harvested on day 5 after onplant grafting and processed for quantitative human-specific *Alu*-qPCR as described (Minder et al., 2015).

CAM tumor model to study spontaneous metastasis

To analyze the effects of purified NE, NC and intact neutrophils on intratumoral angiogenesis and tumor cell intravasation, CAM microtumor assays was employed as described (Deryugina, 2016). Briefly, GFP-tagged HEp3 cells were suspended at $1x10^7$ cells per mL within 2.2 mg/mL neutralized native type I collagen (BD Biosciences). Six 15 µL-droplets of cell-containing collagen mixtures were placed separately on the top of a CAM on 10 day-old chick embryos developing *ex ovo* (Deryugina and Quigley, 2008b). Developing tumors were treated daily by topical application of tested ingredients in PBS supplemented with 1% DMSO (vehicle). Purified NE was used at 100 nM, the NC was used at a concentration equivalent to 100 nM of NE activity, and α1PI was used at a final concentration of 300 nM. To assay the effect of intact neutrophils, freshly isolated neutrophils were injected on day 3 of microtumor development into the allantoic vein of chick embryos ($2x10^6$ neutrophils per embryo). After 5 days, 100 µg of Rhodamine-LCA in PBS was inoculated within 0.1 mL PBS in an allantoic vein to highlight chick embryo vasculature. Within 10-30 minutes, the portions of the CAM distal to tumors were excised and processed for *Alu*-qPCR to determine the number of intravasated human cells, after which the CAM microtumors were imaged using an Olympus IX51 microscope equipped with a QuantiFire XI digital microscope camera. Images were acquired at the original magnification of 200X (20X objective and 10X eyepiece). In acquired images, intratumoral vasculature was analyzed using ImageJ for lumen size distribution. The lumen diameters were determined for 3-5 areas within a tumor, 2-6 tumors per embryo, 3-5 embryos per group, allowing for statistically significant number of measurements.

Pulmonary tumor cell arrest and lung retention in mice

Lung retention experiments were conducted as described (Oncogene, 2012). WT and NE-KO mice (6-to-8-week-old) were injected through a lateral tail vein with $5x10^5$ HEp3 cells or $1x10^6$ PC3 cells per mouse. Both sexes of mice were used throughout the study, although one the mice of one sex of similar age were used in an individual experiment. Tumor cell arrest in pulmonary vasculature and lung tissue retention of tumor cells was analyzed correspondingly after 30 minutes or 12 hours following cell inoculations. Where indicated, the mice following cell injections were treated with Sivelestat at 1-1.5 mg/kg administered up to three times in 0.2 mL PBS/4%DMSO i.p. or i.v. during 12-hr-long duration of lung retention assays. Control. Mice were treated with vehicle (PBS/4% DMSO). Lung tissue was harvested and processed for human-specific *Alu*-qPCR to determine actual numbers of human cells using a standard curve as described (Conn et al., 2009; Deryugina and Kiosses, 2017; Minder et al., 2015).

Mouse orthotopic model for spontaneous metastasis of head and neck cancer

Mouse model to study mechanisms of spontaneous metastasis of head and neck cancer was performed as described (Deryugina et al., 2018). Herein, we employed an aggressive murine head and neck carcinoma cell line, MOC2, a syngeneic setting using genetically compatible C57BL/6 mice, WT and NE KO. Both sexes of mice were used throughout the study, although

one the mice of one sex of similar age were used in an individual experiment. MOC2 cells were inoculated into buccal lining of the upper lip at 1×10^6 per site (one site per mouse). After 12-14 days, mice were sacrificed when primary tumors reached end point-size of ~0.5 cm in diameter. Tumors were excised and weighed. Lungs (the major organ for hematogenous dissemination of head and neck carcinomas in this model) were harvested and fixed for histological examination. Lung sections were stained with hematoxylin-eosin and digitally scanned. Areas in the lung tissue occupied by tumor cells were outlined and quantified using ImageJ software.

Quantitative human-specific Alu-qPCR

Dissemination of human tumor cells in CAM or mouse assays was measured by the quantification of human-specific *Alu* repeats in total DNA extracted from host tissue as described (Conn et al., 2009; Deryugina and Kiosses, 2017; Minder et al., 2015). The DNA was purified using the Puregene DNA purification kit from Qiagen. The *Alu*-qPCR was performed on 10 ng of genomic DNA in a Bio-Rad MyIQ LightCycler (Bio-Rad) using SYBR green (Life Technologies) as a binding dye. The Cq values were converted into number of human cells using a standard curve generated by spiking increasing numbers of human tumor cells (from 10 to 10^4 cells) into a fixed number (10^6 cells) of chick embryo fibroblasts or murine B16 melanoma cells.

Statistical analysis

Data were analyzed using GraphPad Prism 7 (GraphPad Software, La Jolla, CA). In bar graphs the data are presented as mean ± SEM from either a representative experiment or several normalized pooled experiments. To normalize the data, the ratios of numerical values for each measurement over the mean of the control group of an individual experiment were calculated. The outliers were eliminated based on the Grubb's test incorporated in GraphPad Software. The differences (*P* values) between data sets were analyzed with the unpaired two-tailed Student's *t*-test. *P* values <0.05 were considered statistically significant.

Supplemental References

Conn, E.M., Botkjaer, K.A., Kupriyanova, T.A., Andreasen, P.A., Deryugina, E.I., and Quigley, J.P. (2009). Comparative analysis of metastasis variants derived from human prostate carcinoma cells: roles in intravasation of VEGF-mediated angiogenesis and uPA-mediated invasion. Am J Pathol *175*, 1638-1652.

Deryugina, E.I. (2016). Chorioallantoic Membrane Microtumor Model to Study the Mechanisms of Tumor Angiogenesis, Vascular Permeability, and Tumor Cell Intravasation. Methods Mol Biol *1430*, 283-298.

Deryugina, E.I., and Kiosses, W.B. (2017). Intratumoral Cancer Cell Intravasation Can Occur Independent of Invasion into the Adjacent Stroma. Cell Reports *19*, 601-616.

Deryugina, E.I., and Quigley, J.P. (2008a). Chapter 2. Chick embryo chorioallantoic membrane models to quantify angiogenesis induced by inflammatory and tumor cells or purified effector molecules. Methods Enzymol *444*, 21-41.

Deryugina, E.I., and Quigley, J.P. (2008b). Chick embryo chorioallantoic membrane model systems to study and visualize human tumor cell metastasis. Histochem Cell Biol *130*, 1119-1130.

Deryugina, E.I., Zajac, E., Zilberberg, L., Muramatsu, T., Joshi, G., Dabovic, B., Rifkin, D., and Quigley, J.P. (2018). LTBP3 promotes early metastatic events during cancer cell dissemination. Oncogene *37*, 1815-1829.

Judd, N.P., Winkler, A.E., Murillo-Sauca, O., Brotman, J.J., Law, J.H., Lewis, J.S., Jr., Dunn, G.P., Bui, J.D., Sunwoo, J.B., and Uppaluri, R. (2012). ERK1/2 regulation of CD44 modulates oral cancer aggressiveness. Cancer Research *72*, 365-374.

Minder, P., Zajac, E., Quigley, J.P., and Deryugina, E.I. (2015). EGFR regulates the development and microarchitecture of intratumoral angiogenic vasculature capable of sustaining cancer cell intravasation. Neoplasia *17*, 634-649.

Toolan, H.W. (1954). Transplantable human neoplasms maintained in cortisone-treated laboratory animals: H.S. No. 1; H.Ep. No. 1; H.Ep. No. 2; H.Ep. No. 3; and H.Emb.Rh. No. 1. Cancer Research *14*, 660-666.